Inorg. Chem. **2005**, *44*, 9471–9488

Solution Self-Assembly, Spontaneous Deprotonation, and Crystal Structures of Bipyrazolate-Bridged Metallomacrocycles with Dimetal Centers†

Shu-Yan Yu,*[,‡,||] Hai-Ping Huang,[‡] Sheng-Hui Li,[‡] Qing Jiao,[‡] Yi-Zhi Li,*[,§] Biao Wu,[⊥] Yoshihisa Sei,[#] Kentaro Yamaguchi,*[,#] Yuan-Jiang Pan,[⊗] and Hong-Wei Ma[‡]

State Key Laboratory of Polymer Physics and Chemistry, Institute of Chemistry, and Graduate School of the Chinese Academy of Sciences, Beijing 100080, People's Republic of China, State Key Laboratory of Coordination Chemistry, Institute of Coordination Chemistry, Nanjing University, Nanjing 210093, People's Republic of China, Laboratory for Self-Assembly Chemistry, Department of Chemistry, Renmin University of China, Beijing 100872, People's Republic of China, State Key Laboratory of Oxo Synthesis & Selective Oxidation, Lanzhou Institute of Chemical Physics, Chinese Academy of Sciences, Lanzhou 730000, People's Republic of China, Laboratory of Analytical Chemistry, Department of Pharmaceutical Technology, Faculty of Pharmaceutical Sciences at Kagawa Campus, Tokushima Bunri University, Shido, Sanuki-city, Kagawa 769-2193, Japan, and Department of Chemistry, Zhejiang University, Hangzhou 310027, People's Republic of China

Received June 9, 2005

A series of nanosized cavity-containing bipyrazolate-bridged metallomacrocycles with dimetal centers, namely, $\{[(bpy)M]_8L_4\}(NO_3)_8$ [L = 3,3′,5,5′-tetramethyl-4,4′-bipyrazolyl, Pd **1**, Pt **2**; 1,4-bis-4′-(3′,5′-dimethyl)-pyrazolylbenzene), Pd **5**; and 1,4-bis-4′-(3′,5′-dimethyl)-pyrazolylbiphenyl, Pd **9]**, $\{[(phen)M]_8L_4\}(NO_3)_8$ [L = 3,3′,5,5′-tetramethyl-4,4′-bipyrazolyl, Pd **3**, Pt **4**; 1,4-bis-4′-(3′,5′-dimethyl)-pyrazolylbenzene, Pd **7**; and 1,4-bis-4′-(3′,5′-dimethyl)-pyrazolylbiphenyl, Pd **11**], $\{[(bpy)Pd]_6L_3\}(NO_3)_6$ [L = 1,4-bis-4′-(3′,5′-dimethyl)-pyrazolylbenzene, **6**, **10]**, $\{[(phen)Pd]_6L_3\}(NO_3)_6$ [L = 1,4-bis-4′-(3′,5′-dimethyl)-pyrazolylbenzene, **8**, **12]**, $\{[(bpy)Pd]_4L_2\}(NO_3)_4$ [L = 1,3-bis-4′-(3′,5′-dimethyl)-pyrazolylbenzene, **13**, and 1,2-bis-4′-(3′,5′-dimethyl)-pyrazolylbenzene, **15**], and $\{[(phen)Pd]_4L_2\}(NO_3)_4$ [L = 1,3-bis-4′-(3′,5′-dimethyl)-pyrazolylbenzene, **14**, and 1,2-bis-4′-(3′,5′-dimethyl)-pyrazolylbenzene, **16**] (where bpy = 2,2′-bipyridine and phen = 1,10-phenanthroline) have been synthesized through a directed self-assembly approach that involves spontaneous deprotonation of the 1*H*-bipyrazolyl ligands in aqueous solution. These complexes, with weak Pd(II)···Pd(II) or Pt(II)···Pt(II) interactions, have been characterized by elemental analysis, ^{1}H and ^{13}C NMR, cold-spray ionization or electrospray ionization mass spectrometry, UV–visible spectroscopy, and luminescence spectroscopy. Complexes **1**, **3**, **5**, **6**, **14**, and **15** have also been characterized by single-crystal X-ray diffraction analysis.

Introduction

Over the past decade, the synthetic approach via metal-directed self-assembly[1−3] has led to the rapid development of supramolecular coordination compounds with a variety of geometrically and topologically elegant structures such as molecular triangles,[3,4,6−8] squares and rectangles,[3,5−10] pentagons and hexagons,[11] bowls and cages,[12] cuboctahedra and dodecahedra,[13] helicates, grids, catenanes, nanotubes and polytubes,[14] and so on. These metallosupramolecular systems have displayed attractive properties in molecular recognition and catalysis,[3,6,12,13] redox activity,[3,9,10] magnetism, luminescence, and electron transfer.[9,10,15] Recently, we have been interested in the design and self-assembly of structurally and functionally new metallomacrocycles, such as molecular bowls, capsules, crowns, and baskets, that function as anion

† Dedicated to Prof. Dr. F. Albert Cotton.

* To whom correspondence should be addressed. E-mail: syu@iccas.ac.cn (S.-Y.Y.), llyyjz@nju.edu.cn (Y.-Z.L., for X-ray structure crystallography), yamaguchi@kph.bunri-u.ac.jp (K.Y., for CSI-MS analysis). Fax: +86-10-62559373 (S.-Y.Y.).

‡ Chinese Academy of Sciences.

§ Nanjing University.

|| Renmin University of China.

⊥ Lanzhou Institute of Chemical Physics.

Tokushima Bunri University.

⊗ Zhejiang University (for NMR and ESI-MS analysis).

10.1021/ic0509332 CCC: $30.25
Published on Web 11/05/2005

receptors and for molecular encapsulation.[3b,12,16] However, it remains a great challenge to make an appropriate choice of coordination motifs as building blocks for de novo design to control the "retro-assembly (synthesis) analysis" approach to nanoscale inorganic supramolecular self-assembly. By far, most of the metallosupramolecular systems have been built upon only a few kinds of coordination motifs, namely, the motifs of uncoordinated (naked) single metal ions with a variety of chelating ligands, which have been comprehensively developed by Lehn, Sauvage, Saalfrank, and Raymond, whereas the precoordinated or uncoordinated square-planar Pd(II) or Pt(II) has been introduced by Fujita and Stang and the octahedral Re(I) has been introduced by Hupp with monodentate ligands such as bi- or polypyridines. Since 1999, Cotton and co-workers have pioneered the utilization of metal−metal-bonded dimetal units as corners and the bidentate ligands, such as di- or polycarboxylate,[3e] as linkers for well-defined finite molecular architecture.

In our search for new coordination motifs with specific functions, we noticed that the versatile ligands, 1*H*-bipyrazoles, could be good alternatives for the widely used carboxylates or other bidentate chelating ligands in binding dimetal centers. In view of the variety of potential applications of pyrazolate-bridged multi-metal coordination com-

(1) Lehn, J.-M. *Supramolecular Chemistry, Concepts and Perspectives*; VCH: Weinheim, Germany, 1995.

(2) (a) *Science* **2002**, *295*, 2395−2421 (Supramolecular Chemistry and Self-Assembly, Special Issue). (b) Lindoy, L. F.; Atkinson, I. In *Self-Assembly in Supramolecular Systems (Monographs in Supramolecular Chemistry)*; Stoddart, J. F., Ed.; The Royal Society of Chemistry: London, 2000. (c) Fujita, M. *Molecular Self-Assembly Organic versus Inorganic Approach (Structure and Bonding)*; Springer: New York, 2000; Vol. 96. (d) Sauvage, J.-P. *Transition Metals in Supramolecular Chemistry, Perspectives in Supramolecular Chemistry*; Wiley: New York, 1999; Vol. 5. (e) Lehn, J.-M. Templating, Self-Assembly, and Self-Organization. In *Comprehensive Supramolecular Chemistry*; Sauvage, J.-P., Hosseini, M. W., Eds.; Pergamon: New York, 1996.

(3) (a) Fujita, M.; Tominaga, M.; Hori, A.; Therrien, B. *Acc. Chem. Res.* **2005**, *38*, 371−380. (b) Yu, S.-Y.; Li, S.-H.; Huang, H.-P.; Zhang, Z.-X.; Jiao, Q.; Shen, H.; Hu, X.-X.; Huang, H. *Curr. Org. Chem.* **2005**, *9*, 555−563. (c) Würthner, F.; You, C.-C.; Saha-Möller, C. R. *Chem. Soc. Rev.* **2004**, *33*, 133−146. (d) Seidel, S. R.; Stang, P. J. *Acc. Chem. Res.* **2002**, *35*, 972−983. (e) Cotton, F. A.; Lin, C.; Murillo, C. A. *Acc. Chem. Res.* **2001**, *34*, 759−771. (f) Dinolfo, P. H.; Hupp, J. T. *Chem. Mater.* **2001**, *13*, 3113−3125. (g) Leininger, S.; Olenyuk, B.; Stang, P. J. *Chem. Rev.* **2000**, *100*, 853−908. (h) Caulder, D. L.; Raymond, K. N. *Acc. Chem. Res.* **1999**, *32*, 975−982. (i) Navarro, J. A. R.; Lippert, B. *Coord. Chem. Rev.* **1999**, *185*−*186*, 653−667. (j) Fujita, M. *Acc. Chem. Res.* **1999**, *32*, 53−61. (k) Fujita, M. *Chem. Soc. Rev.* **1998**, *27*, 417−425. (l) Slone, R. V.; Benkstein, K. D.; Bélanger, S.; Hupp, J. T.; Guzei, I. A.; Rheingold, A. L. *Coord. Chem. Rev.* **1998**, *171*, 221−243. (m) Stang, P. J. *Chem.*−*Eur. J.* **1998**, *4*, 19−27. (n) Stang, P. J.; Olenyuk, B. *Acc. Chem. Res.* **1997**, *30*, 502−518. (o) Fujita, M.; Ogura, K. *Coord. Chem. Rev.* **1996**, *148*, 249−264.

(4) (a) Schnebeck, R.-D.; Freisinger, E.; Glahe, F.; Lippert, B. *J. Am. Chem. Soc.* **2000**, *122*, 1381−1390. (b) Schnebeck, R.-D.; Freisinger, E.; Lippert, B. *Chem. Commun.* **1999**, 675−676. (c) Schnebeck, R.-D.; Randaccio, L.; Zangrando, E.; Lippert, B. *Angew. Chem., Int. Ed.* **1998**, *37*, 119−121.

(5) (a) Cotton, F. A.; Lei, P.; Lin, C.; Murillo, C. A.; Wang, X.; Yu, S.-Y.; Zhang, Z.-X. *J. Am. Chem. Soc.* **2004**, *126*, 1518−1525. (b) Angaridis, P.; Berry, J. F.; Cotton, F. A.; Murillo, C. A.; Wang, X. *J. Am. Chem. Soc.* **2003**, *125*, 10327−10334. (c) Bera, J. K.; Angaridis, P.; Cotton, F. A.; Petrukhina, M. A.; Fanwick, P. E.; Walton, R. A. *J. Am. Chem. Soc.* **2001**, *123*, 1515−1516. (d) Cotton, F. A.; Daniels, L. M.; Lin, C.; Murillo, C. A.; Yu, S.-Y. *J. Chem. Soc., Dalton Trans.* **2001**, *121*, 502−504. (e) Cotton, F. A.; Daniels, L. M.; Lin, C.; Murillo, C. A. *J. Am. Chem. Soc.* **1999**, *121*, 4538−4539.

(6) (a) Fujita, M.; Sasaki, O.; Mitsuhashi, T.; Fujita, T.; Yazaki, J.; Yamaguchi, K.; Ogura, K. *Chem. Commun.* **1996**, 1535−1536. (b) Fujita, M.; Yazaki, J.; Ogura, K. *J. Am. Chem. Soc.* **1990**, *112*, 5645−5647.

(7) (a) Habereder, T.; Warchhold, M.; Nöth, H.; Severin, K. *Angew. Chem., Int. Ed.* **1999**, *38*, 3225−3228. (b) Lai, S.-W.; Chan, M. C.-W.; Peng, S.-M.; Che, C.-M. *Angew. Chem., Int. Ed.* **1999**, *38*, 669−671. (c) Thompson, A.; Rettig, S. J.; Dolphin, D. *Chem. Commun.* **1999**, 631−632. (d) Hall, J.; Loeb, S. J.; Shimizu, G. K. H.; Yap, G. P. A. *Angew. Chem., Int. Ed.* **1998**, *37*, 121−123. (e) Barbera, J.; Elduque, A.; Gimenez, R.; Oro, L. A.; Serrano, J. L. *Angew. Chem., Int. Ed. Engl.* **1996**, *35*, 2832−2835.

(8) (a) Graves, C. R.; Merlau, M. L.; Morris, G. A.; Sun, S.-S.; Nguyen, S. T.; Hupp, J. T. *Inorg. Chem.* **2004**, *43*, 2013−2017. (b) Ferrer, M.; Mounir, M.; Rossell, O.; Ruiz, E.; Maestro, M. A. *Inorg. Chem.* **2003**, *42*, 5890−5899. (c) Schweiger, M.; Seidel, S. R.; Arif, A. M.; Stang, P. J. *Inorg. Chem.* **2002**, *41*, 2556−2559. (d) Sautter, A.; Schmid, D. G.; Jung, G.; Würthner, F. *J. Am. Chem. Soc.* **2001**, *123*, 5424−5430. (e) Schnebeck, R.-D.; Freisinger, E.; Lippert, B. *Eur. J. Inorg. Chem.* **2000**, 1193−1200. (f) Sun, S.-S.; Lees, A. J. *J. Am. Chem. Soc.* **2000**, *122*, 8956−8967. (g) Sun, S.-S.; Lees, A. J. *Inorg. Chem.* **1999**, *38*, 4181−4182. (h) Lee, S. B.; Hwang, S.; Chung, D. S.; Yun, H.; Hong, J.-I. *Tetrahedron Lett.* **1998**, *39*, 873−876. (i) McQuillan, F. S.; Berridge, T. E.; Chen, H.; Hamor, T. A.; Jones, C. J. *Inorg. Chem.* **1998**, *37*, 4959−4970. (j) Fujita, M.; Ogura, K. *Bull. Chem. Soc. Jpn.* **1996**, *69*, 1471−1482.

(9) (a) Würthner, F.; Sautter, A.; Schmid, D. G.; Weber, P. J. A. *Chem.*−*Eur. J.* **2001**, *7*, 894−902. (b) Sun, S.-S.; Silva, A. S.; Brinn, I. M.; Lees, A. J. *Inorg. Chem.* **2000**, *39*, 1344−1345. (c) Würthner, F.; Sautter, A. *Chem. Commun.* **2000**, 445−446. (d) Lahav, M.; Gabai, R.; Shipway, A. N.; Willner, I. *Chem. Commun.* **1999**, 1937−1938. (e) Campos-Fernandez, C. S.; Clerac, R.; Dunbar, K. R. *Angew. Chem., Int. Ed.* **1999**, *38*, 3477−3479. (f) Woessner, S. M.; Helms, J. B.; Houlis, J. F.; Sullivan, B. P. *Inorg. Chem.* **1999**, *38*, 4380−4381. (g) Slone, R. V.; Hupp, J. T.; Stern, C.; Albrecht-Schmitt, T. E. *Inorg. Chem.* **1996**, *35*, 4096−4097. (h) Slone, R. V.; Yoon, D. I.; Calhoun, R. M.; Hupp, J. T. *J. Am. Chem. Soc.* **1995**, *117*, 11813−11814. (i) Stang, P. J.; Cao, D. H.; Saito, S.; Arif, A. M. *J. Am. Chem. Soc.* **1995**, *117*, 6273−6283. (j) Stang, P. J.; Cao, D. H. *J. Am. Chem. Soc.* **1994**, *116*, 4981−4982.

(10) (a) Hartmann, H.; Berger, S.; Winter, R.; Fiedler, J.; Kaim, W. *Inorg. Chem.* **2000**, *39*, 4977−4980. (b) Benkstein, K. D.; Hupp, J. T.; Stern, C. L. *J. Am. Chem. Soc.* **1998**, *120*, 12982−12983. (c) Benkstein, K. D.; Hupp, J. T.; Stern, C. L. *Angew. Chem., Int. Ed.* **2000**, *39*, 2891−2893. (d) Woessner, S. M.; Helms, J. B.; Shen, Y.; Sullivan, B. P. *Inorg. Chem.* **1998**, *37*, 5406−5407. (e) Benkstein, K. D.; Hupp, J. T.; Stern, C. L. *Inorg. Chem.* **1998**, *37*, 5404−5405.

(11) (a) Matsumoto, N.; Motoda, Y.; Matsuo, T.; Nakashima, T.; Re, N.; Dahan, F.; Tuchagues, J.-P. *Inorg. Chem.* **1999**, *38*, 1165−1173. (b) Mamula, O.; von Zelewsky, A.; Bernardinelli, G. *Angew. Chem., Int. Ed.* **1998**, *37*, 289−293. (c) Stang, P. J.; Persky, N. E.; Manna, J. *J. Am. Chem. Soc.* **1997**, *119*, 4777−4778. (d) Hasenknopf, B.; Lehn, J.-M.; Baum, G.; Kneisel, B. O.; Fenske, D. *Angew. Chem., Int. Ed. Engl.* **1996**, *35*, 1838−1840.

(12) (a) Tashiro, S.; Tominaga, M.; Kawano, M.; Therrien, B.; Ozeki, T.; Fujita, M. *J. Am. Chem. Soc.* **2005**, *127*, 4546−4547. (b) Kusukawa, T.; Fujita, M. *J. Am. Chem. Soc.* **2002**, *124*, 13576−13582. (c) Yu, S.-Y.; Kusukawa, T.; Biradha, K.; Fujita, M. *J. Am. Chem. Soc.* **2000**, *122*, 2665−2666. (d) Fujita, M.; Fujita, N.; Ogura, K.; Yamaguchi, K. *Nature* **1999**, *400*, 52−55. (e) Fujita, M.; Yu, S.-Y.; Kusukawa, T.; Funaki, H.; Ogura, K.; Yamaguchi, K. *Angew. Chem., Int. Ed.* **1998**, *37*, 2082−2085.

(13) (a) Olenyuk, B.; Levin, M. D.; Whiteford, J. A.; Shield, J. E.; Stang, P. J. *J. Am. Chem. Soc.* **1999**, *121*, 10434−10435. (b) Olenyuk, B.; Whiteford, J. A.; Fechtenkötter, A.; Stang, P. J. *Nature* **1999**, *398*, 796−799. (c) Takeda, N.; Umemoto, K.; Yamaguchi, K.; Fujita, M. *Nature* **1999**, *398*, 794−796.

(14) (a) Yamaguchi, T.; Tashiro, S.; Tominaga, M.; Kawano, M.; Ozeki, T.; Fujita, M. *J. Am. Chem. Soc.* **2004**, *126*, 10818−10819. (b) Biradha, K.; Aoyagi, M.; Fujita, M. *J. Am. Chem. Soc.* **2000**, *122*, 2397−2398. (c) Aoyagi, M.; Biradha, K.; Fujita, M. *J. Am. Chem. Soc.* **1999**, *121*, 7457−7458.

(15) (a) Iengo, E.; Milani, B.; Zangrando, E.; Geremia, S.; Alessio, E. *Angew. Chem., Int. Ed.* **2000**, *39*, 1096−1099. (b) Drain, C. M.; Nifiatis, F.; Vasenko, A.; Batteas, J. D. *Angew. Chem., Int. Ed.* **1998**, *37*, 2344−2347. (c) Funatsu, K.; Imamura, T.; Ichimura, A.; Sasaki, Y. *Inorg. Chem.* **1998**, *37*, 1798−1804. (d) Slone, R. V.; Hupp, J. T. *Inorg. Chem.* **1997**, *36*, 5422−5423. (e) Drain, C. M.; Lehn, J.-M. *J. Chem. Soc., Chem. Commun.* **1994**, 2313−2315.

(16) (a) Yu, S.-Y.; Huang, H.; Liu, H.-B.; Chen, Z.-N.; Zhang, R.; Fujita, M. *Angew. Chem., Int. Ed.* **2003**, *42*, 686−690. (b) Li, S.-H.; Huang, H.-P.; Yu, S.-Y.; Li, Y.-Z.; Huang, H.; Sei, Y.; Yamaguchi, K. *Dalton Trans.* **2005**, 2346−2348.

pounds in catalysis, biological mimicry, magnetic coupling, electron transfer, and photophysical studies,[17−22] we have started the self-assembly of metallomacrocycles with bi- or polypyrazolyl ligands.[23] To the best of our knowledge, only a handful of dinuclear or polynuclear palladium(II) or platinum(II) complexes with simple pyrazolate-bridged ligands have been documented in the literature so far.[21] Similarly, the 1*H*-bipyrazoles have rarely been utilized in molecular self-assembly to date,[23] although some infinite solid structures[24] formed through hydrogen bonding and coordination have recently been reported in the field of crystal engineering. Furthermore, the use of bipyrazolate-linked dimetal centers in the preparation of metallomacrocyclic molecular architectures has not been reported to date.

Here we describe the solution self-assembly and structural characterization of a series of metallomacrocyclic complexes with dipalladium(II) or diplatinum(II) centers and bipyrazolate dianion linkers. These molecular assemblies have been intensively studied by NMR spectroscopy, by electrospray ionization mass spectrometry (ESI-MS) or cold-spray ionization mass spectrometry (CSI-MS)[25] in solution and by X-ray crystallographic analysis in the solid state. The photophysical properties (electronic absorption and luminescence) of the complexes in solution have also been discussed. Furthermore, the spontaneous deprotonation of 1*H*-bipyrazoles in the solution self-assembly processes has been investigated by NMR and pH-coordination titration, which represents a facile approach from mononuclear coordination compounds to supramolecular architectures with dimetal coordination motifs.

Experimental Section

Materials. Potassium hexafluorophosphate (99%) and sodium tetrafluoroborate (99%) were purchased from Acros Organics and used without further purification. Methanol for photophysical experiments was of spectroscopic grade. All other chemicals and solvents were of reagent grade and were purified according to conventional methods.[26] The compounds (bpy)Pd$(NO_3)_2$, (bpy)Pt$(NO_3)_2$, (phen)Pd$(NO_3)_2$, and (phen)Pt$(NO_3)_2$ (where bpy = 2,2′-bipyridine and phen = 1,10-phenanthroline) were prepared according to literature procedures.[27,28] The bipyrazole ligands 3,3′,5,5′-tetramethyl-4,4′-bipyrazolyl (H_2L^1),[29] 1,4-bis-4′-(3′,5′-dimethyl)-pyrazolylbenzene (H_2L^2),[30] 1,4-bis-4′-(3′,5′-dimethyl)-pyrazolylbiphenyl (H_2L^3),[30] 1,3-bis-4′-(3′,5′-dimethyl)-pyrazolylbenzene (H_2L^4),[30] and 1,2-bis-4′-(3′,5′-dimethyl)-pyrazolylbenzene (H_2L^5)[30] were synthesized according to the published methods.

Instrumentation. ^{1}H and ^{13}C NMR experiments were performed on a Bruker DMX300, a Bruker Avance DMX400, and a Bruker DMX500 spectrometer using tetramethylsilane (TMS) as an internal standard. CSI-MS spectra were recorded with a four-sector (BE/BE) tandem mass spectrometer (JMS-700T, JEOL) equipped with a CSI source. ESI-MS measurements were performed with an HP5989B mass spectrometer. Elemental analyses were performed on a Thermoquest Flash EA 1112 instrument. UV−visible absorption spectra were obtained on a Shimadzu UV-1601 PC spectrophotometer. Luminescence spectra were measured on a Hitachi F-4500 fluorescence spectrophotometer. The pH titration experiments were performed on a Hanna pH 211 microprocessor-based bench pH/mV/°C meter.

Synthesis. Two of the bipyrazole ligands, 1,4-bis-4′-(3′,5′-dimethyl)-pyrazolylbiphenyl (H_2L^3) and 1,3-bis-4′-(3′,5′-dimethyl)-pyrazolylbenzene (H_2L^4), are new compounds and were synthesized using a method similar to that employed for the other known ligands.[30]

1,4-Bis-4′-(3′,5′-dimethyl)-pyrazolylbiphenyl (H_2L^3). Mp >300 °C. ^{1}H NMR (300 MHz, DMSO-d_6, 25 °C, TMS, ppm): 12.30 (br s, 2H, NH), 7.73 (d, J = 8.3 Hz, 4H), 7.39 (d, J = 8.2 Hz, 4H), 2.27 (s, 12H, CH_3). Anal. Calcd for $C_{22}H_{22}N_4$ (%): C, 77.16; H, 6.48; N, 16.36. Found: C, 76.68; H, 6.74; N, 16.21.

1,3-Bis-4′-(3′,5′-dimethyl)-pyrazolylbenzene) (H_2L^4). Mp 230 °C. ^{1}H NMR (400 MHz, DMSO-d_6, 25 °C, TMS, ppm): 12.30 (br s, 2H, NH), 7.40 (t, J = 7.5 Hz, 1H, Ar−H_5), 7.14 (d, J = 7.5 Hz, 2H, Ar−$H_{4,6}$), 7.13 (s, 1H, Ar−H_2), 2.21 (s, 12H, CH_3). ^{13}C NMR (100.6 MHz, DMSO-d_6, δ): 134.6, 129.4, 129.0, 126.5, 117.3,

(17) Cotton, F. A.; Walton, R. A. *Multiple Bonds Between Metal Atoms*; Oxford University Press: Oxford, 1993.

(18) (a) Shiu, K.-B.; Lee, H.-C.; Lee, G.-H.; Ko, B. T.; Wang, Y.; Lin, C.-C. *Angew. Chem., Int. Ed.* **2003**, *42*, 2999−3001. (b) Shiu, K.-B.; Lee, H.-C.; Lee, G.-H.; Wang, Y. *Organometallics* **2002**, *21*, 4013−4016. (c) Süss-Fink, G.; Wolfender, J.-L.; Neumann, F.; Stoeckli-Evans, H. *Angew. Chem., Int. Ed. Engl.* **1990**, *29*, 429−431.

(19) La Monica, G.; Ardizzoia, G. A. In *Progress in Inorganic Chemistry*, Karlin, K. D., Ed.; Wiley: New York, 1997; Vol. 46, pp 151−238.

(20) (a) Ma, B.; Li, J.; Djurovich, P. I.; Yousufuddin, M.; Bau, R.; Thompson, M. E. *J. Am. Chem. Soc.* **2005**, *127*, 28−29. (b) Lu, W.; Chan, M. C. W.; Zhu, N.; Che, C.-M.; Li, C.; Hui, Z. *J. Am. Chem. Soc.* **2004**, *126*, 7639−7651. (c) Lai, S.-W.; Chan, M. C.-W.; Cheung, T.-C.; Peng, S.-M.; Che, C.-M. *Inorg. Chem.* **1999**, *38*, 4046−4055.

(21) (a) Huang, H.-P.; Li, S.-H.; Yu, S.-Y.; Li, Y.-Z.; Jiao, Q.; Pan, Y.-J. *Inorg. Chem. Commun.* **2005**, *8*, 656−660. (b) Umakoshi, K.; Yamauchi, Y.; Nakamiya, K.; Kojima, T.; Yamasaki, M.; Kawano, H.; Onishi, M. *Inorg. Chem.* **2003**, *42*, 3907−3916. (c) Boixassa, A.; Pons, J.; Solans, X.; Font-Bardia, M.; Ros, J. *Inorg. Chem. Commun.* **2003**, *6*, 922−925. (d) Pons, J.; Chadghan, A.; Casabó, J.; Alvarez-Larena, A.; Piniella, J. F.; Ros, J. *Inorg. Chem. Commun.* **2000**, *3*, 296−299. (e) Sakai, K.; Sato, T.; Tsubomura, T.; Matsumoto, K. *Acta Crystallogr., Sect. C* **1996**, *52*, 783−786.

(22) (a) Yam, V. W.-W.; Hui, C.-K.; Yu, S.-Y.; Zhu, N.-Y. *Inorg. Chem.* **2004**, *43*, 812−821. (b) Yam, V. W.-W.; Wong, K. M.-C.; Zhu, N. *J. Am. Chem. Soc.* **2002**, *124*, 6506−6507.

(23) Zhang, Z.-X.; Huang, H.; Yu, S.-Y. *Chin. J. Inorg. Chem.* **2004**, *20*, 849−852 (and references therein).

(24) (a) Boldog, I.; Rusanov, E. B.; Sieler, J.; Domasevitch, K. V. *New J. Chem.* **2004**, *28*, 756−759. (b) Boldog, I.; Sieler, J.; Domasevitch, K. V. *Inorg. Chem. Commun.* **2003**, *6*, 769−772. (c) Boldog, I.; Rusanov, E. B.; Sieler, J.; Blaurock, S.; Domasevitch, K. V. *Chem. Commun.* **2003**, 740−741. (d) Ponomarova, V. V.; Komarchuk, V. V.; Boldog, I.; Chernega, A. N.; Sieler, J.; Domasevitch, K. V. *Chem. Commun.* **2002**, 436−437. (e) Boldog, I.; Sieler, J.; Chernega, A. N.; Domasevitch, K. V. *Inorg. Chim. Acta* **2002**, *338*, 69−77. (f) Boldog, I.; Rusanov, E. B.; Chernega, A. N.; Sieler, J.; Domasevitch, K. V. *Angew. Chem., Int. Ed.* **2001**, *40*, 3435−3438. (g) Boldog, I.; Rusanov, E. B.; Chernega, A. N.; Sieler, J.; Domasevitch, K. V. *J. Chem. Soc., Dalton Trans.* **2001**, 893−897. (h) Boldog, I.; Rusanov, E. B.; Chernega, A. N.; Sieler, J.; Domasevitch, K. V. *Polyhedron* **2001**, *20*, 887−897. (i) Kruger, P. E.; Moubaraki, B.; Fallon, G. D.; Murray, K. S. *J. Chem. Soc., Dalton Trans.* **2000**, 713−718. (j) Cuadro, A.; Elguero, J.; Santos, P. N. R. *Inorg. Chim. Acta* **1984**, *80*, 99−105.

(25) (a) Yamaguchi, K. *J. Mass Spectrom.* **2003**, *38*, 473−490. (b) Sakamoto, S.; Nakatani, K.; Saito, I.; Yamaguchi, K. *Chem. Commun.* **2003**, 788−789. (c) Sakamoto, S.; Yoshizawa, M.; Kusukawa, T.; Fujita, M.; Yamaguchi, K. *Org. Lett.* **2001**, *3*, 1601−1604. (d) Sakamoto, S.; Fujita, M.; Kim, K.; Yamaguchi, K. *Tetrahedron* **2000**, *56*, 955−964.

(26) Armarego, W. L. F.; Perrin, D. D. *Purification of Laboratory Chemicals*, 4th ed.; Butterworth Heinemann: Oxford, 1997.

(27) Yu, S.-Y.; Fujita, M.; Yamaguchi, K. *J. Chem. Soc., Dalton Trans.* **2001**, 3419−3420 (and references therein).

(28) Conrad, R. C.; Rund, J. V. *Inorg. Chem.* **1972**, *11*, 129−134.

(29) Kruger, P. E.; Moubaraki, B.; Fallon, G. D.; Murray, K. S. *J. Chem. Soc., Dalton Trans.* **2000**, 713−718.

(30) (a) Ramirez, F.; Bhatia, S. B.; Patwardhan, A. V.; Smith, C. P. *J. Org. Chem.* **1967**, *32*, 2194−2199. (b) Ramirez, F.; Bhatia, S. B.; Patwardhan, A. V.; Smith, C. P. *J. Org. Chem.* **1967**, *32*, 3547−3553.

11.8−12.3 (br, s). Anal. Calcd for $C_{16}H_{18}N_4$ (%): C, 72.15; H, 6.81; N, 21.04. Found: C, 71.71; H, 6.92; N, 21.16.

{[(bpy)Pd]$_8$L$^1_4$}(NO$_3$)$_8$ (1). (bpy)Pd(NO$_3$)$_2$ (92.8 mg, 0.24 mmol) was added to a suspension of H_2L^1 (22.8 mg, 0.12 mmol) in H_2O (12 mL), and the mixture was stirred for 2 h at room temperature. The resulting clear yellow solution was evaporated to dryness to give a yellow solid. Pure **1**, as a microcrystalline yellow solid, was obtained by the vapor diffusion of diethyl ether into a 2 mM solution of **1** in methanol at room temperature. Yield: 99.5 mg (99%). ^{1}H NMR (400 MHz, acetone-d_6/D_2O = 2:1, 25 °C, TMS, ppm): 8.65 (d, J = 8.2 Hz, 8H), 8.61 (d, J = 8.2 Hz, 8H), 8.54 (d, J = 5.3 Hz, 8H), 8.43−8.52 (m, 24H), 7.83 (t, J = 6.4 Hz, 8H), 7.78 (t, J = 6.3 Hz, 8H), 2.50 (s, 24H, CH_3), 2.14 (s, 24H, CH_3). ^{13}C NMR (150.9 MHz, acetone-d_6/D_2O = 2:1, 25 °C, ppm): 157.7, 152.3, 151.5, 150.3, 144.1, 129.9, 125.7, 112.9, 13.8 (CH_3). UV/visible (methanol, ϵ, M^{-1} cm^{-1}, λ_{max}, nm): 237 (181 900), 309 (87 220), 321 (sh, 71 830), 364 (8930), 383 (sh, 4800). Emission (methanol, λ_{max}, nm): 407. Anal. Calcd for $C_{120}H_{112}N_{40}O_{24}Pd_8{\cdot}4H_2O$ (%): C, 42.12; H, 3.53; N, 16.37. Found: C, 42.07; H, 3.68; N, 16.26. CSI-MS (methanol, m/z): 1612.4 [**1** − 2NO$_3^-$]$^{2+}$, 1054.1 [**1** − 3NO$_3^-$]$^{3+}$, 774.9 [**1** − 4NO$_3^-$]$^{4+}$, 608.2 [**1** − 5NO$_3^-$]$^{5+}$, 495.8 [**1** − 6NO$_3^-$]$^{6+}$, 416.4 [**1** − 7NO$_3^-$]$^{7+}$, 357.1 [**1** − 8NO$_3^-$]$^{8+}$.

The BF_4^- salt of **1** (**1a**) was obtained by adding a 10-fold excess of $NaBF_4$ to its aqueous solution at 60 °C, which resulted in the immediate deposition of **1a** as yellow microcrystals in quantitative yield. The crystals were filtered, washed with a minimum amount of cold water, and dried under vacuum. ^{1}H NMR (400 MHz, CD_3-CN, 25 °C, ppm): 8.39 (d, J = 7.9 Hz, 8H), 8.35 (d, J = 7.6 Hz, 8H), 8.23−8.32 (m, 24H), 8.20 (d, J = 5.4 Hz, 8H), 7.71 (t, J = 6.6 Hz, 8H), 7.64 (t, J = 6.5 Hz, 8H), 2.36 (s, 24H, CH_3), 2.16 (s, 24H, CH_3). Anal. Calcd for $C_{120}H_{112}N_{32}B_8F_{32}Pd_8{\cdot}10H_2O$ (%): C, 38.66; H, 3.57; N, 12.02. Found: C, 38.42; H, 3.42; N, 12.17. X-ray quality crystals were grown by the vapor diffusion of diethyl ether into a 1.0 mM solution of **1a** in acetonitrile at room temperature.

{[(bpy)Pt]$_8$L$^1_4$}(NO$_3$)$_8$ (2). (bpy)Pt(NO$_3$)$_2$ (90.1 mg, 0.20 mmol) was added to a suspension of H_2L^1 (19.0 mg, 0.10 mmol) in H_2O (10 mL), and the mixture was stirred for 24 h at 90 °C. The resulting clear yellow solution was evaporated to dryness to give a yellow solid. Pure **2**, as a microcrystalline yellow solid, was obtained by the same method as used for **1**. Yield: 100.5 mg (99%). ^{1}H NMR (400 MHz, acetone-d_6/D_2O = 2:1, 25 °C, TMS, ppm): 8.88 (d, J = 5.5 Hz, 8H), 8.82 (d, J = 5.5 Hz, 8H), 8.68 (d, J = 7.8 Hz, 8H), 8.61 (d, J = 8.2 Hz, 8H), 8.56 (t, J = 7.5 Hz, 8H), 8.50 (t, J = 7.9 Hz, 8H), 7.92 (t, J = 6.6 Hz, 8H), 7.88 (t, J = 6.9 Hz, 8H), 2.50 (s, 24H, CH_3), 2.04 (s, 24H, CH_3). UV/visible (methanol, ϵ, M^{-1} cm^{-1}, λ_{max}, nm): 247 (114 580), 311 (69 430), 321 (68 830), 363 (21 780), 420 (sh, 3650). Emission (methanol, λ_{max}, nm): 406. Anal. Calcd for $C_{120}H_{112}N_{40}O_{24}Pt_8{\cdot}12H_2O$ (%): C, 33.71; H, 3.21; N, 13.10. Found: C, 33.45; H, 3.13; N, 13.18. ESI-MS (methanol, m/z): 1290.9 [**2** − 3NO$_3^-$]$^{3+}$, 952.7 [**2** − 4NO$_3^-$]$^{4+}$, 749.8 [**2** − 5NO$_3^-$]$^{5+}$, 614.5 [**2** − 6NO$_3^-$]$^{6+}$.

{[(phen)Pd]$_8$L$^1_4$}(NO$_3$)$_8$ (3). The same procedure as employed for **1** was followed for the synthesis of **3**, except that (phen)Pd-(NO$_3$)$_2$ (98.6 mg, 0.24 mmol) was used as the starting material. Yield: 103.1 mg (97%). ^{1}H NMR (400 MHz, acetone-d_6/D_2O = 2:1, 25 °C, TMS, ppm): 9.07 (d, J = 8.3 Hz, 8H), 8.98 (d, J = 5.2 Hz, 8H), 8.94 (d, J = 8.4 Hz, 8H), 8.90 (d, J = 5.3 Hz, 8H), 8.36 (s, 8H), 8.21 (dd, J_1 = 8.4 Hz, J_2 = 5.4 Hz, 8H), 8.20 (s, 8H), 8.12 (dd, J_1 = 8.4 Hz, J_2 = 5.4 Hz, 8H), 2.71 (s, 24H, CH_3), 2.28 (s, 24H, CH_3). ^{13}C NMR (150.9 MHz, acetone-d_6/D_2O = 2:1, 25 °C, ppm): 153.6, 152.1, 150.9, 1748.3, 147.9, 142.8, 132.4, 129.5, 128.3, 113.2, 14.1 (CH_3). UV/visible (methanol, ϵ, M^{-1} cm^{-1}, λ_{max}, nm): 222 (411 320), 275 (261 240), 353 (31 420), 383 (sh, 12 540). Emission (methanol, λ_{max}, nm): 417. Anal. Calcd for $C_{136}H_{112}N_{40}O_{24}$-$Pd_8{\cdot}8H_2O$ (%): C, 44.31; H, 3.77; N, 15.20. Found: C, 44.26; H, 3.62; N, 15.07. CSI-MS (methanol, m/z): 1709.1 [**3** − 2NO$_3^-$]$^{2+}$, 1118.5 [**3** − 3NO$_3^-$]$^{3+}$, 823.2 [**3** − 4NO$_3^-$]$^{4+}$, 646.3 [**3** − 5NO$_3^-$]$^{5+}$, 527.7 [**3** − 6NO$_3^-$]$^{6+}$, 443.6 [**3** − 7NO$_3^-$]$^{7+}$, 380.6 [**3** − 8NO$_3^-$]$^{8+}$.

The PF_6^- salt of **3** (**3a**) was prepared by exchange with a 10-fold excess of KPF_6 in aqueous solution. ^{1}H NMR (400 MHz, CD_3-CN, 25 °C, ppm): 8.89 (dd, J_1 = 8.3 Hz, J_2 = 1.1 Hz, 8H), 8.68 (dd, J_1 = 8.3 Hz, J_2 = 1.1 Hz, 8H), 8.65 (dd, J_1 = 5.3 Hz, J_2 = 1.1 Hz, 8H), 8.50 (dd, J_1 = 5.3 Hz, J_2 = 1.1 Hz, 8H), 8.22 (s, 8H), 8.03 (dd, J_1 = 8.3 Hz, J_2 = 5.3 Hz, 8H), 8.00 (s, 8H), 7.87 (dd, J_1 = 8.3 Hz, J_2 = 5.3 Hz, 8H), 2.55 (s, 24H, CH_3), 2.08 (s, 24H, CH_3). Anal. Calcd for $C_{136}H_{112}N_{32}P_8F_{48}Pd_8$ (%): C, 38.84; H, 2.68; N, 10.66. Found: C, 38.47; H, 2.67; N, 10.75. X-ray quality crystals were grown by the vapor diffusion of diethyl ether into a 1.0 mM solution of **3a** in acetonitrile at room temperature.

{[(phen)Pt]$_8$L$^1_4$}(NO$_3$)$_8$ (4). The same procedure as employed for **2** was followed for the synthesis of **4**, except that (phen)Pt-(NO$_3$)$_2$ (99.9 mg, 0.20 mmol) was used as the starting material. Yield: 104.2 (98%). ^{1}H NMR (400 MHz, acetone-d_6/D_2O = 2:1, 25 °C, TMS, ppm): 9.31 (d, J = 5.1 Hz, 8H), 9.22 (d, J = 5.1 Hz, 8H), 9.15 (d, J = 8.3 Hz, 8H), 9.02 (d, J = 8.3 Hz, 8H), 8.39 (s, 8H), 8.27 (dd, J_1 = 8.1 Hz, J_2 = 5.6 Hz, 8H), 8.25 (s, 8H), 8.16 (dd, J_1 = 8.1 Hz, J_2 = 5.3 Hz, 8H), 2.71 (s, 24H, CH_3), 2.18 (s, 24H, CH_3). UV/visible (methanol, ϵ, M^{-1} cm^{-1}, λ_{max}, nm): 225 (251 760), 276 (204 320), 361 (26 680), 372 (29 060), 420 (sh, 2680). Emission (methanol, λ_{max}, nm): 417. Anal. Calcd for $C_{136}H_{112}N_{40}O_{24}Pt_8{\cdot}8H_2O$ (%): C, 37.16; H, 2.94; N, 12.75. Found: C, 37.02; H, 2.86; N, 12.58. ESI-MS (methanol, m/z): 1355.0 [**4** − 3NO$_3^-$]$^{3+}$, 1000.7 [**4** − 4NO$_3^-$]$^{4+}$, 788.2 [**4** − 5NO$_3^-$]$^{5+}$, 646.5 [**4** − 6NO$_3^-$]$^{6+}$.

{[(bpy)Pd]$_8$L$^2_4$}(NO$_3$)$_8$ (5) and {[(bpy)Pd]$_6$L$^2_3$}(NO$_3$)$_6$ (6). (bpy)Pd(NO$_3$)$_2$ (85.1 mg, 0.22 mmol) was added to a suspension of H_2L^2 (29.3 mg, 0.11 mmol) in H_2O (10 mL) and acetone (1 mL), and the mixture was stirred for 2 h at room temperature. The resulting clear yellow solution was evaporated to dryness to give a yellow solid. This was identified by NMR spectroscopy as a mixture of **5** and **6** (80:20). Pure **6**, as yellow thick needlelike crystals, was separated by repeated recrystallizations through the vapor diffusion of diethyl ether into a 2 mM solution of the mixture in methanol at room temperature, and the residual villiform crystals were pure **5**. **5.** Yield: 80.4 mg (80%). ^{1}H NMR (400 MHz, acetone-d_6/D_2O = 1:10, 25 °C, TMS, ppm): 8.68 (d, J = 8.5 Hz, 16H, bpy-H$_{6,6'}$), 8.51 (t, J = 8.0 Hz, 16H, bpy-H$_{5,5'}$), 8.47 (d, J = 5.5 Hz, 16H, bpy-H$_{3,3'}$), 7.87 (t, J = 6.7 Hz, 16H, bpy-H$_{4,4'}$), 7.50 (s, 16H, Ar−H), 2.64 (s, 48H, CH_3). ^{13}C NMR (75.5 MHz, acetone-d_6/D_2O = 1:10, 25 °C, ppm): 155.2, 149.6, 145.8, 141.3, 129.8, 127.7, 127.0, 123.0, 119.3, 11.6 (CH_3). CSI-MS (methanol, m/z): 1765.7 [**5** − 2NO$_3^-$]$^{2+}$, 1156.4 [**5** − 3NO$_3^-$]$^{3+}$, 851.7 [**5** − 4NO$_3^-$]$^{4+}$, 669.0 [**5** − 5NO$_3^-$]$^{5+}$, 547.7 [**5** − 6NO$_3^-$]$^{6+}$, 461.0 [**5** − 7NO$_3^-$]$^{7+}$, 394.8 [**5** − 8NO$_3^-$]$^{8+}$. Anal. Calcd for $C_{144}H_{128}N_{40}O_{24}Pd_8{\cdot}8H_2O$ (%): C, 45.53; H, 3.82; N, 14.75. Found: C, 45.69; H, 4.01; N, 14.89. **6.** Yield: 20.1 mg (20%). ^{1}H NMR (400 MHz, acetone-d_6/D_2O = 1:10, 25 °C, TMS, ppm): 8.68 (d, J = 8.1 Hz, 12H, bpy-H$_{6,6'}$), 8.60 (d, J = 5.3 Hz, 12H, bpy-H$_{3,3'}$), 8.52 (t, J = 7.9 Hz, 12H, bpy-H$_{5,5'}$), 7.89 (t, J = 6.6 Hz, 12H, bpy-H$_{4,4'}$), 7.38 (s, 12H, Ar−H), 2.62 (s, 36H, CH_3). ^{13}C NMR (100.6 MHz, CD_3OD, 25 °C, ppm): 156.9, 150.8, 149.1, 142.1, 131.4, 129.1, 127.9, 124.0, 121.3, 12.1 (CH_3). CSI-MS (methanol, m/z): 1308.1 [**6** − 2NO$_3^-$]$^{2+}$, 851.4 [**6** − 3NO$_3^-$]$^{3+}$, 622.8 [**6** − 4NO$_3^-$]$^{4+}$, 485.8 [**6** − 5NO$_3^-$]$^{5+}$, 394.9

Table 1. Crystallographic Data for Complexes **1a**, **3a**, **5a**, **6a**, **14a**, and **15**

	1a·8H_2O	**3a**·13H_2O	**5a**·6CH_3CN·6H_2O	**6a**·16H_2O	**14a**·12H_2O	**15**·8H_2O
empirical formula	$C_{120}H_{128}B_8F_{32}N_{32}O_8Pd_8$	$C_{136}H_{138}F_{48}N_{32}O_{13}P_8Pd_8$	$C_{156}H_{158}F_{48}N_{38}O_6P_8Pd_8$	$C_{108}H_{128}F_{36}N_{24}O_{16}P_6Pd_6$	$C_{80}H_{88}F_{24}N_{16}O_{12}P_4Pd_4$	$C_{72}H_{80}N_{20}O_{20}Pd_4$
fw	3692.22	4439.74	4672.16	3526.56	2471.14	1971.16
cryst syst, space group	monoclinic, *C*2/*c*	monoclinic, *P*2/*c*	triclinic, $P\bar{1}$	orthorhombic, *Pnma*	orthorhombic, *Pnma*	orthorhombic, *Ibam*
a, Å	19.493(5)	18.398(16)	12.454(2)	20.228(4)	23.444(6)	18.463(4)
b, Å	38.151(4)	20.61(2)	22.437(4)	32.832(6)	38.640(9)	20.759(4)
c, Å	25.291(7)	31.038(16)	27.684(5)	26.962(5)	13.633(3)	22.208(4)
α, deg	90.00	90.00	77.492(4)	90.00	90.00	90.00
β, deg	110.948(4)	117.59(3)	78.918(4)	90.00	90.00	90.00
γ, deg	90.00	90.00	82.733(4)	90.00	90.00	90.00
V, Å^3	17 565(7)	10 431(15)	7382(2)	17 906(6)	12 350(5)	8512(3)
Z	4	2	1	4	4	4
ρ_{calcd}, g cm^{-3}	1.396	1.414	1.051	1.308	1.329	1.538
μ, mm^{-1}	0.886	0.831	0.589	0.732	0.712	0.910
F(000)	7328	4404	2328	7048	4944	3984
transm range	0.75−0.80	0.77−0.82	0.87−0.89	0.81−0.85	0.81−0.84	0.77−0.85
θ range, deg	1.72−26.00	0.99−26.00	1.87−25.50	0.98−28.00	1.81−26.00	1.48−26.00
no. data	17 249	20 528	26 855	21 633	12 268	4302
no. params	1004	1204	1260	1031	728	282
GOF[a]	1.052	0.981	1.046	0.992	1.065	1.089
R1, wR2 [$I > 2\sigma(I)$][b]	0.0504, 0.1134	0.0528, 0.1069	0.0639, 0.1575	0.0639, 0.1224	0.0615, 0.1076	0.0559, 0.1143
R1, wR2 (all data)[b]	0.0720, 0.1186	0.0794, 0.1121	0.0958, 0.1660	0.1053, 0.1297	0.0958, 0.1134	0.0802, 0.1195

[a] GOF = $\{\sum[w(F_o^2 - F_c^2)^2]/(n-p)\}^{1/2}$, where *n* and *p* denote the number of data points and the number of parameters, respectively. [b] R1 = $(\sum||F_o| - |F_c||)/\sum|F_o|$; wR2 = $\{\sum[w(F_o^2 - F_c^2)^2]/\sum[w(F_o^2)^2]\}^{1/2}$, where $w = 1/[\sigma^2(F_o^2) + (aP)^2 + bP]$ and $P = [\max(0,F_o^2) + 2F_c^2]/3$.

[**6** − 6NO_3^-]$^{6+}$. Anal. Calcd for $C_{108}H_{96}N_{30}O_{18}Pd_6$·6$H_2O$ (%): C, 45.54; H, 3.82; N, 14.75. Found: C, 45.59; H, 3.81; N, 14.97.

The PF_6^- salts of **5** and **6** (**5a** and **6a**) were prepared by exchange with a 10-fold excess of KPF_6 in aqueous solution. **5a**. ^{1}H NMR (400 MHz, CD_3CN, 25 °C, ppm): 8.40 (t, J = 8.2 Hz, 16H, bpy-$H_{6,6'}$), 8.33 (d, J = 6.6 Hz, 16H, bpy-$H_{5,5'}$), 8.23 (d, J = 5.4 Hz, 16H, bpy-$H_{3,3'}$), 7.73 (t, J = 6.7 Hz, 16H, bpy-$H_{4,4'}$), 7.51 (s, 16H, Ar−H), 2.56 (s, 48H, CH_3). Anal. Calcd for $C_{144}H_{128}N_{32}P_8F_{48}Pd_8$·6$H_2O$·3$CH_3CN$ (%): C, 39.60; H, 3.30; N, 10.78. Found: C, 39.64; H, 3.19; N, 10.65. **6a**. ^{1}H NMR (400 MHz, CD_3CN, 25 °C, ppm): 8.30−8.50 (m, 36H), 7.70 (t, J = 6.7 Hz, 12H, bpy-$H_{4,4'}$), 7.32 (s, 12H, Ar−H), 2.53 (s, 36H, CH_3). Anal. Calcd for $C_{108}H_{96}N_{24}P_6F_{36}Pd_8$·4$H_2O$ (%): C, 39.18; H, 3.17; N, 10.15. Found: C, 39.01; H, 3.07; N, 10.16. X-ray quality crystals were grown by the vapor diffusion of diethyl ether into a 1.0 mM solution of the PF_6^- salts of **5a** or **6a** in acetonitrile at room temperature.

{[(phen)Pd]$_8$L$^2_4$}(NO$_3$)$_8$ (7) and {[(phen)Pd]$_6$L$^2_3$}(NO$_3$)$_6$ (8). The same procedure as employed for **5** and **6** was followed for the synthesis of **7** and **8**, except that (phen)Pd$(NO_3)_2$ (90.4 mg, 0.22 mmol) was used as the starting material. The resulting yellow solid was identified by NMR spectroscopy as a mixture of **7** and **8** (75:25). Pure **8** (yellow needles) and **7** (villiform crystals) could be separated using a similar method as for **6** and **5**. **7.** Yield: 79.4 mg (75%). ^{1}H NMR (400 MHz, acetone-d_6/D_2O = 1:10, 25 °C, TMS, ppm): 9.07 (d, J = 8.3 Hz, 16H, phen-$H_{2,9}$), 8.89 (d, J = 5.2 Hz, 16H, phen-$H_{4,7}$), 8.35 (s, 16H, phen-$H_{5,6}$), 8.20 (dd, J_1 = 8.2 Hz, J_2 = 5.3 Hz, 16H, phen-$H_{3,8}$), 7.64 (s, 16H, Ar−H), 2.79 (s, 48H, CH_3). ^{13}C NMR (100.6 MHz, acetone-d_6/D_2O = 1:10, 25 °C, ppm): 150.3, 146.3, 145.5, 140.1, 129.8, 129.6, 127.8, 126.6, 125.3, 119.4, 11.0 (CH_3). CSI-MS (methanol, *m*/*z*): 1220.3 [**7** − 3NO_3^-]$^{3+}$, 899.5 [**7** − 4NO_3^-]$^{4+}$, 707.0 [**7** − 5NO_3^-]$^{5+}$, 578.5 [**7** − 6NO_3^-]$^{6+}$. Anal. Calcd for $C_{160}H_{128}N_{40}O_{24}Pd_8$·10$H_2O$ (%): C, 47.73; H, 3.71; N, 13.91. Found: C, 47.65; H, 3.86; N, 13.55. **8**. Yield: 26.5 mg (25%). ^{1}H NMR (400 MHz, acetone-d_6/D_2O = 1:10, 25 °C, TMS, ppm): 9.08 (d, J = 8.3 Hz, 12H, phen-$H_{2,9}$), 9.00 (d, J = 5.1 Hz, 12H, phen-$H_{4,7}$), 8.36 (s, 12H, phen-$H_{5,6}$), 8.21 (dd, J_1 = 8.1 Hz, J_2 = 5.5 Hz, 12H, phen-$H_{3,8}$), 7.50 (s, 12H, Ar−H), 2.76 (s, 36H, CH_3). ^{13}C NMR (100.6 MHz, CD_3OD, 25 °C, ppm): 151.4, 149.5, 147.2, 140.8, 131.4, 131.0, 129.2, 127.6, 126.2, 121.4, 12.3 (CH_3).

Chart 1

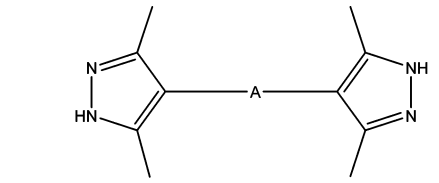

A

H_2L^1: none

H_2L^2:

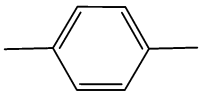

H_2L^3:

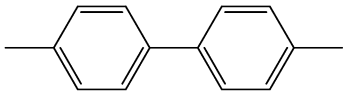

H_2L^4:

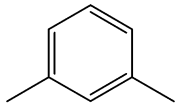

H_2L^5:

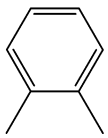

CSI-MS (methanol, *m*/*z*): 1380.5 [**8** − 2NO_3^-]$^{2+}$, 899.7 [**8** − 3NO_3^-]$^{3+}$, 659.0 [**8** − 4NO_3^-]$^{4+}$, 515.0 [**8** − 5NO_3^-]$^{5+}$, 418.7 [**8** − 6NO_3^-]$^{6+}$. Anal. Calcd for $C_{120}H_{96}N_{30}O_{18}Pd_6$·6$H_2O$ (%): C, 48.16; H, 3.64; N, 14.04. Found: C, 48.21; H, 3.56; N, 14.14.

{[(bpy)Pd]$_8$L$^3_4$}(NO$_3$)$_8$ (9) and {[(bpy)Pd]$_6$L$^3_3$}(NO$_3$)$_6$ (10). Reaction of (bpy)Pd$(NO_3)_2$ (46.4 mg, 0.12 mmol) and H_2L^3 (20.5 mg, 0.06 mmol) in H_2O/acetone (10:1 mL) for 12 h at 50 °C afforded a mixture of **9** and **10** (47:53) as a yellow solid. All

Scheme 1

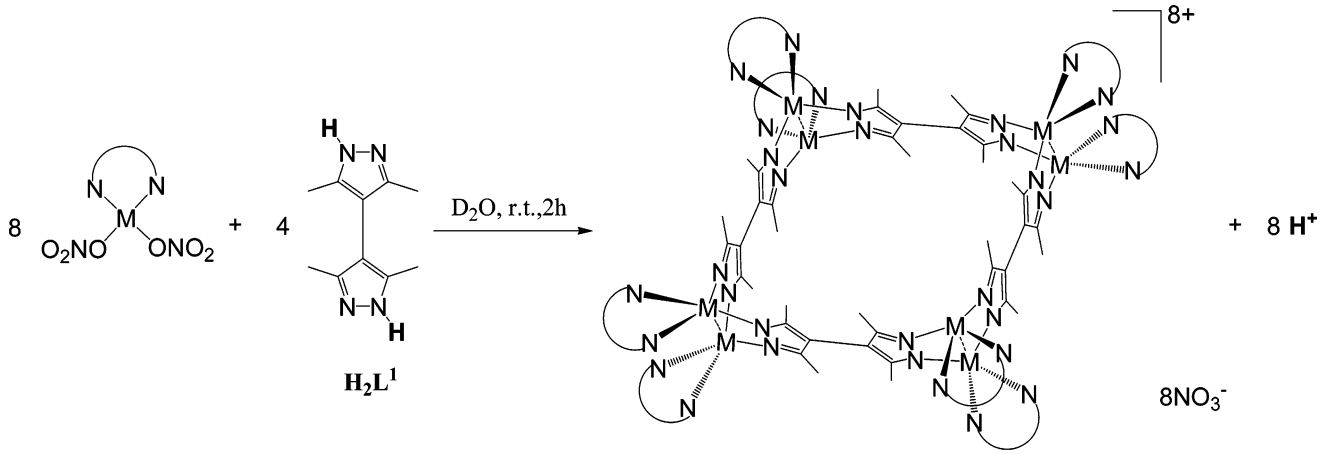

(bpy)Pd(NO$_3$)$_2$ **1**

(bpy)Pt(NO$_3$)$_2$ **2**

(phen)Pd(NO$_3$)$_2$ **3**

(phen)Pt(NO$_3$)$_2$ **4**

attempts to separate the mixture by repeated recrystallizations were unsuccessful as a result of the poor solubility of the compounds. Yield: 58.8 mg (99%). ^{1}H NMR (400 MHz, DMSO-d_6, 25 °C, TMS, ppm): 8.76 (d, J = 8.3 Hz, bpy-H$_{6,6'}$), 8.48 (t, J = 7.3 Hz, bpy-H$_{5,5'}$), 8.37 [d, J = 5.1 Hz, bpy-H$_{3,3'}$ (**10**)], 8.45 [d, J = 4.9 Hz, bpy-H$_{3,3'}$ (**9**)], 7.7−7.9 (m, bpy-H$_{4,4'}$ and biPh-H), 7.53 [d, J = 7.7 Hz (**9**)], 7.42 [d, J = 8.0 Hz (**10**)], 2.54 [s, 48H, CH$_3$ (**9**)], 2.52 [s, 36H, CH$_3$ (**10**)]. CSI-MS (methanol, *m*/*z*): 1422.7 [**10** − 2NO$_3^-$]$^{2+}$, 1258.0 [**9** − 3NO$_3^-$]$^{3+}$, 928.2 [**9** − 4NO$_3^-$]$^{4+}$ and [**10** − 3NO$_3^-$]$^{3+}$, 730.0 [**9** − 5NO$_3^-$]$^{5+}$, 680.4 [**10** − 4NO$_3^-$]$^{4+}$, 598.2 [**9** − 6NO$_3^-$]$^{6+}$, 531.9 [**10** − 5NO$_3^-$]$^{5+}$, 503.6 [**9** − 7NO$_3^-$]$^{7+}$, 433.0 [**9** − 8NO$_3^-$]$^{8+}$ and [**10** − 6NO$_3^-$]$^{6+}$.

{[(phen)Pd]$_8$L$^3_4$}(NO$_3$)$_8$ (11) and {[(phen)Pd]$_6$L$^3_3$}(NO$_3$)$_6$ (12). The same procedure as employed for **9** and **10** was followed for the synthesis of **11** and **12**, except that (phen)Pd(NO$_3$)$_2$ (49.3 mg, 0.12 mmol) was used as the starting material, which afforded a mixture of **11** and **12** (47:53). The pure compounds of **11** and **12** also cannot be isolated by repeated recrystallizations as a result of their poor solubility. Yield: 61.6 mg (99%). ^{1}H NMR (400 MHz, DMSO-d_6, 25 °C, TMS, ppm): 9.07 (d, J = 8.0 Hz, phen-H$_{2,9}$), 8.76 [d, J = 5.0 Hz, phen-H$_{4,7}$ (**12**)], 8.65 [d, J = 4.7 Hz, phen-H$_{4,7}$ (**11**)], 8.36 (s, phen-H$_{5,6}$), 8.14 (dd, J_1 = 8.1, J_2 = 5.4 Hz, phen-H$_{3,8}$), 7.90 [d, J = 8.2 Hz (**12**)], 7.81 [d, J = 8.0 Hz (**11**)], 7.63 [d, J = 8.1 Hz (**11**)], 7.50 [d, J = 8.1 Hz (**12**)], 2.66 [s, CH$_3$ (**11**)], 2.64 [s, CH$_3$ (**12**)]. ESI-MS (methanol, *m*/*z*): 975.1 [**11** − 4NO$_3^-$]$^{4+}$ and [**12** − 3NO$_3^-$]$^{3+}$, 768.1 [**11** − 5NO$_3^-$]$^{5+}$, 716.3 [**12** − 4NO$_3^-$]$^{4+}$, 629.8 [**11** − 6NO$_3^-$]$^{6+}$, 560.3 [**12** − 5NO$_3^-$]$^{5+}$, 531.1 [**11** − 7NO$_3^-$]$^{7+}$, 456.6 [**11** − 8NO$_3^-$]$^{8+}$ and [**12** − 6NO$_3^-$]$^{6+}$.

{[(bpy)Pd]$_4$L$^4_2$}(NO$_3$)$_4$ (13). Similar to the above procedures, a reaction of (bpy)Pd(NO$_3$)$_2$ (92.8 mg, 0.24 mmol) and H$_2$L^4 (32.0 mg, 0.12 mmol) in H$_2$O/acetone (8:4 mL) for 2 h yielded **13**. Pure **13**, as a microcrystalline yellow solid, was obtained by recrystallizing from acetone and water. Yield: 106.3 mg (97%). ^{1}H NMR (400 MHz, acetone-d_6/D$_2$O = 1:1, 25 °C, TMS, ppm): 8.63 (2d, J = 6.4 Hz, 16H, bpy-H$_{6,6'}$ and H$_{3,3'}$), 8.51 (t, J = 8.2 Hz, 8H, bpy-H$_{5,5'}$), 7.88 (t, J = 6.7 Hz, 8H, bpy-H$_{4,4'}$), 7.65 (t, J = 7.7 Hz, 2H, Ar−H$_5$), 7.40 (dd, J_1 = 7.7 Hz, J_2 = 1.4 Hz, 4H, Ar−H$_{4,6}$), 6.59 (br s, 2H, Ar−H$_2$), 2.61 (s, 24H, CH$_3$). ^{13}C NMR (100.6 MHz, acetone-d_6/D$_2$O = 1:1, 25 °C, TMS, ppm): 156.3, 150.7, 149.7, 142.6, 133.1, 131.3, 129.4, 128.6, 127.1, 124.2, 121.1, 12.4 (CH$_3$). Anal. Calcd for C$_{72}$H$_{64}$N$_{20}$O$_{12}$Pd$_4$·3H$_2$O(%): C, 45.97; H, 3.75; N, 14.89. Found: C, 46.06; H, 3.72; N, 14.93. The PF$_6^-$ salt, **13a**, was prepared by exchange with a 10-fold excess of KPF$_6$ in aqueous solution. CSI-MS (CH$_3$CN, *m*/*z*): 934.1 [**13a** − 2PF$_6^-$]$^{2+}$, 574.4 [**13a** − 3PF$_6^-$]$^{3+}$, 394.6 [**13a** − 4PF$_6^-$] $^{4+}$.

{[(phen)Pd]$_4$L$^4_2$}(NO$_3$)$_4$ (14). The same procedure as employed for **13** was followed for the synthesis of **14**, except that (phen)Pd(NO$_3$)$_2$ (98.6 mg, 0.24 mmol) was used as the starting material. Yield: 114.2 mg (99%). ^{1}H NMR (400 MHz, acetone-d_6/D$_2$O = 1:1, 25 °C, TMS, ppm): 9.06 (d, J = 8.4 Hz, 8H, phen-H$_{2,9}$), 9.01 (d, J = 5.3 Hz, 8H, phen-H$_{4,7}$), 8.34 (s, 8H, phen-H$_{5,6}$), 8.18 (dd, J_1 = 8.4 Hz, J_2 = 5.3 H, 8H, phen-H$_{3,8}$), 7.70 (t, J = 7.7 Hz, 2H, Ar−H$_5$), 7.50 (dd, J_1 = 7.7 Hz, J_2 = 1.4 Hz, 4H, Ar−H$_{4,6}$), 6.70 (br s, 2H, Ar−H$_2$), 2.72 (s, 24H, CH$_3$). ^{13}C NMR (75.5 MHz, acetone-d_6/D$_2$O = 1:1, 25 °C, TMS, ppm): 151.4, 150.0, 146.5, 141.1, 133.0, 131.4, 130.6, 129.3, 127.7, 127.1, 126.4, 121.2, 12.4 (CH$_3$). Anal. Calcd for C$_{80}$H$_{64}$N$_{20}$O$_{12}$Pd$_4$·2H$_2$O(%): C, 49.04; H, 3.50; N, 14.30. Found: C, 48.96; H, 3.64; N, 14.42. The PF$_6^-$ salt of **14** (**14a**) was prepared by exchange with a 10-fold excess of KPF$_6$ in aqueous solution. CSI-MS (CH$_3$CN, *m*/*z*): 982.1 [**14a** − 2PF$_6^-$]$^{2+}$, 606.4 [**14a** − 3PF$_6^-$]$^{3+}$, 418.8 [**14a** − 4PF$_6^-$]$^{4+}$. X-ray quality crystals were grown by the vapor diffusion of diethyl ether into a 1.0 mM solution of **14a** in acetonitrile.

{[(bpy)Pd]$_4$L$^5_2$}(NO$_3$)$_4$ (15). The same procedure as employed for **13** was followed for the synthesis of **15**, except that H$_2$L^5 (32.0 mg, 0.12 mmol) was used as the starting material. Yield: 108.5 mg (99%). ^{1}H NMR (400 MHz, acetone-d_6/D$_2$O = 1:1, 25 °C, TMS, ppm): 8.62 (d, J = 7.8 Hz, 8H, bpy-H$_{6,6'}$), 8.47 (t, J = 7.8 Hz, 8H, bpy-H$_{5,5'}$), 8.28 (d, J = 5.2 Hz, 8H, bpy-H$_{3,3'}$), 7.85 (t, J = 5.2 Hz, 8H, bpy-H$_{4,4'}$), 7.59 (m, 4H, Ar−H), 7.53 (m, 4H, Ar−H), 2.29 (s, 24H, CH$_3$). ^{13}C NMR (100.6 MHz, acetone-d_6/D$_2$O = 1:1, 25 °C, TMS, ppm): 156.5, 150.8, 146.8, 142.7, 134.2, 133.3, 128.3,

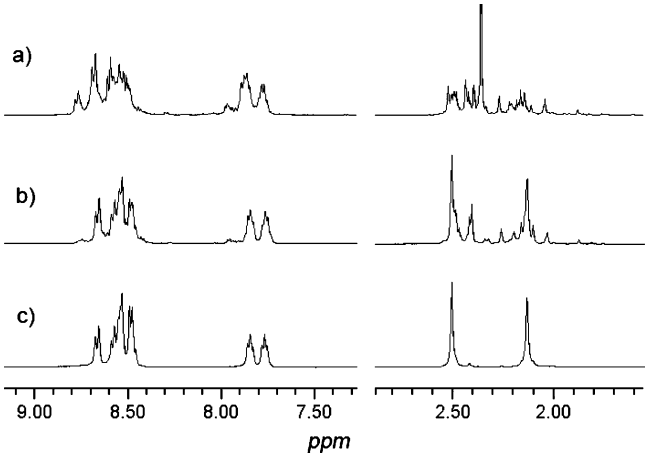

Figure 1. ^{1}H NMR monitoring of the complexation of (bpy)Pd$(NO_3)_2$ to H_2L^1 in D_2O in the aromatic region (left, enlarged) and methyl region (right; 500 MHz, $[H_2L^1] = 10$ mmol L^{-1}, 25 °C): (a) 1:1, (b) 1.5:1, and (c) 2:1.

128.0, 124.3, 121.7, 12.6 (CH_3). Anal. Calcd for $C_{72}H_{64}N_{20}O_{12}Pd_4 \cdot 2H_2O$(%): C, 46.42; H, 3.68; N, 15.04. Found: C, 46.41; H, 3.88; N, 14.90. X-ray quality crystals were grown by the vapor diffusion of diethyl ether into a 1.0 mM solution of **15** in methanol.

{[(phen)Pd]$_4$L$^5_2$}(NO$_3$)$_4$ (16). The same procedure as employed for **13** was followed for the synthesis of **16**, except that (phen)Pd$(NO_3)_2$ (98.6 mg, 0.24 mmol) was used as the starting material. Yield: 111.9 mg (97%). ^{1}H NMR (400 MHz, acetone-d_6/D_2O = 1:1, 25 °C, TMS, ppm): 9.02 (dd, $J_1 = 8.4$ Hz, $J_2 = 1.0$ Hz, 8H, phen-$H_{2,9}$), 8.70 (dd, $J_1 = 5.3$ Hz, $J_2 = 1.0$ Hz, 8H, phen-$H_{4,7}$), 8.31 (s, 8H, phen-$H_{5,6}$), 8.15 (dd, $J_1 = 8.4$ Hz, $J_2 = 5.3$ Hz, 8H, phen-$H_{3,8}$), 7.71 (br s, 8H, Ar−H), 2.47 (s, 24H, CH_3). ^{13}C NMR (100.6 MHz, acetone-d_6/D_2O = 1:1, 25 °C, TMS, ppm): 151.6, 147.2, 146.8, 141.4, 134.4, 133.4, 130.9, 128.2, 128.0, 126.6, 121.9, 12.9 (CH_3). Anal. Calcd for $C_{80}H_{64}N_{20}O_{12}Pd_4 \cdot 2H_2O$(%): C, 49.04; H, 3.50; N, 14.30. Found: C, 49.23; H, 3.48; N, 14.49.

X-ray Structural Determinations. X-ray diffraction measurements were carried out at 293 K on a Bruker Smart Apex charge-coupled device area detector equipped with graphite monochromated Mo Kα radiation ($\lambda = 0.710\ 73$ Å). The absorption correction for all complexes was performed using SADABS. All the structures were solved by direct methods, refined employing full-matrix least-squares on F^2 using the SHELXTL (Bruker, 2000) program, and expanded using Fourier techniques. All of the non-H atoms of the complexes were refined with anisotropic thermal parameters. The hydrogen atoms were included in idealized positions. Final residuals along with unit cell, space group, data collection, and refinement parameters are presented in Table 1.

Results and Discussion

Synthesis of the Bipyrazole Ligands. Chart 1 summarizes the bipyrazole ligands used in this article. The ligands H_2L^1−H_2L^5 were synthesized according to the published procedures.[30] Compounds 1,4-bis-4′-(3′,5′-dimethyl)-pyrazolylbiphenyl (H_2L^3) and 1,3-bis-4′-(3′,5′-dimethyl)-pyrazolylbenzene (H_2L^4) are reported for the first time.

Self-Assembly of Highly Distorted [M$_8$L$_4$]$^{8+}$-Type Macrocycles Based on the Bipyrazole Ligand H$_2$L^1. The self-assembly of bipyrazolate-bridged metallomacrocyclic complexes **1**−**4** is shown in Scheme 1. A mixture of (bpy)M$(NO_3)_2$ or (phen)M$(NO_3)_2$ with H_2L^1 (3,3′,5,5′-tetramethyl-4,4′-bipyrazolyl) in a 2:1 molar ratio in water results in the formation of bipyrazolate-linked metallomacrocyclic complexes {[(bpy)M]$_8$L$^1_4$}$(NO_3)_8$ [M = Pd(II), **1**, M = Pt(II), **2**] or {[(phen)M]$_8$L$^1_4$}$(NO_3)_8$ [M = Pd(II), **3**, M = Pt(II), **4**]

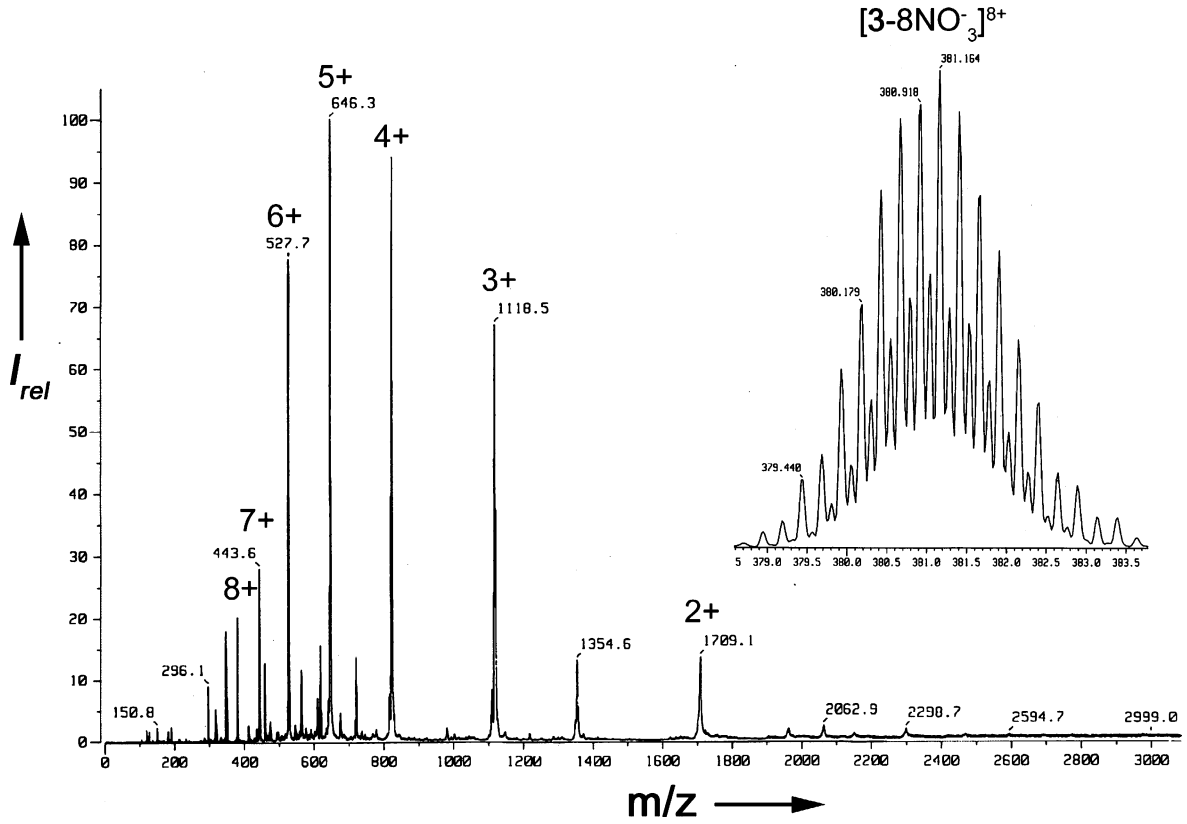

Figure 2. CSI-MS spectrum of **3** in methanol; the inset shows the isotopic distribution of the species [**3** − 8NO_3^-]$^{8+}$.

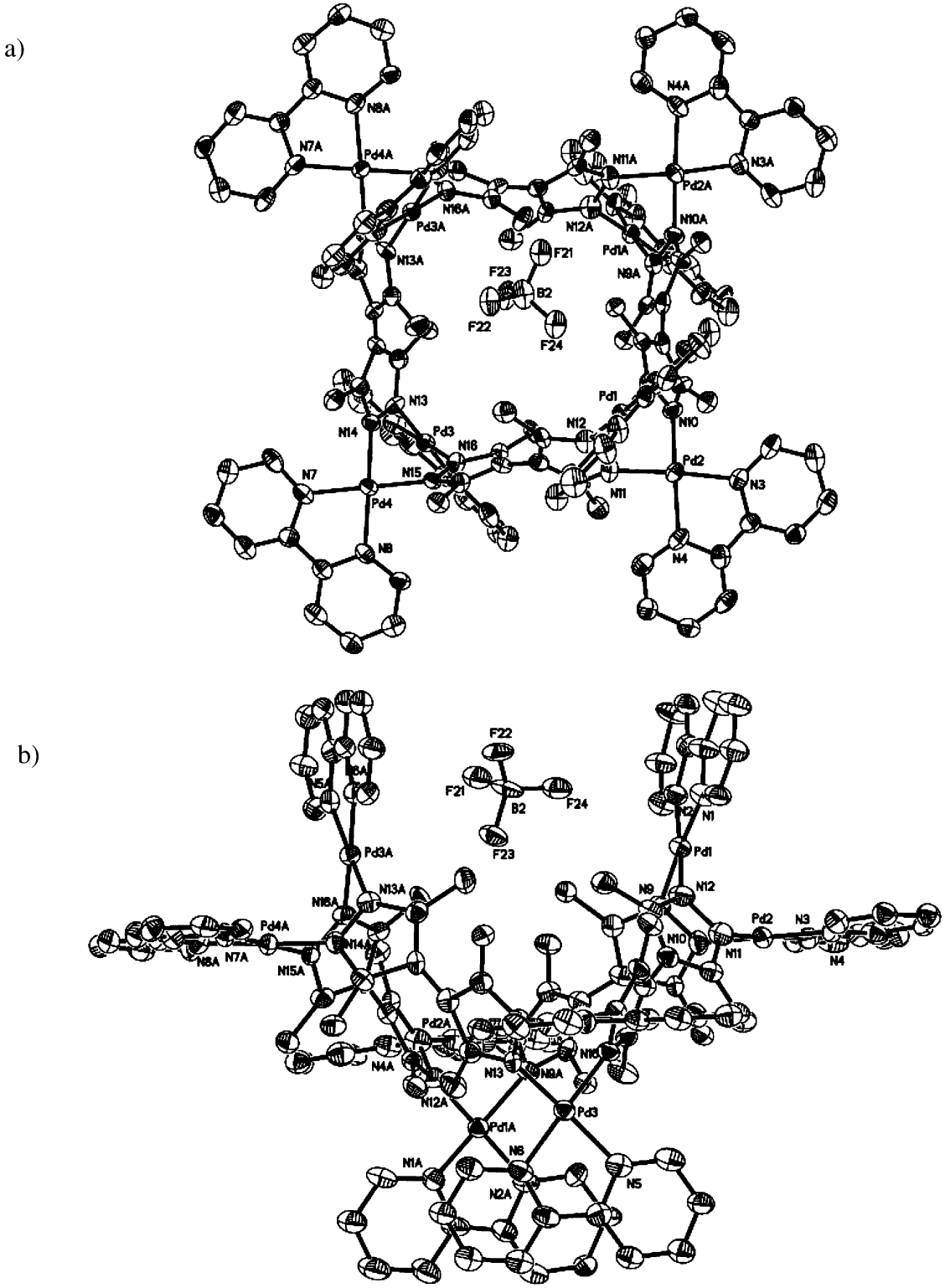

Figure 3. ORTEP diagram of the molecular structure of **1a**: (a) top view and (b) side view. Thermal ellipsoids are shown at the 30% probability level. The remaining counterions and solvent molecules are omitted for clarity.

in quantitative yield with spontaneous deprotonation of H_2L^1. The ^1H and ^{13}C NMR spectra indicate the formation of a single product. The assignments of products **1**−**4** as $[M_8L_4]^{8+}$-type macrocycles are based on CSI-MS and ESI-MS studies, where multiply charged molecular ions corresponding to intact cyclic tetramers were observed. Single-crystal X-ray structural studies of **1a** (the BF_4^- salt of **1**) and **3a** (the PF_6^- salt of **3**) confirmed the formation of the $[M_8L_4]^{8+}$-type macrocycles.

The NMR spectrum of **1** clearly shows that a 2:1 (bpy)Pd to L^1 complex is formed (Figure 1c). Notably, two singlets, at 2.14 and 2.50 ppm with a 1:1 ratio, due to the methyl protons of the bipyrazole ligand are evident in proportion to the protons of two types of bpy in the low-field region of

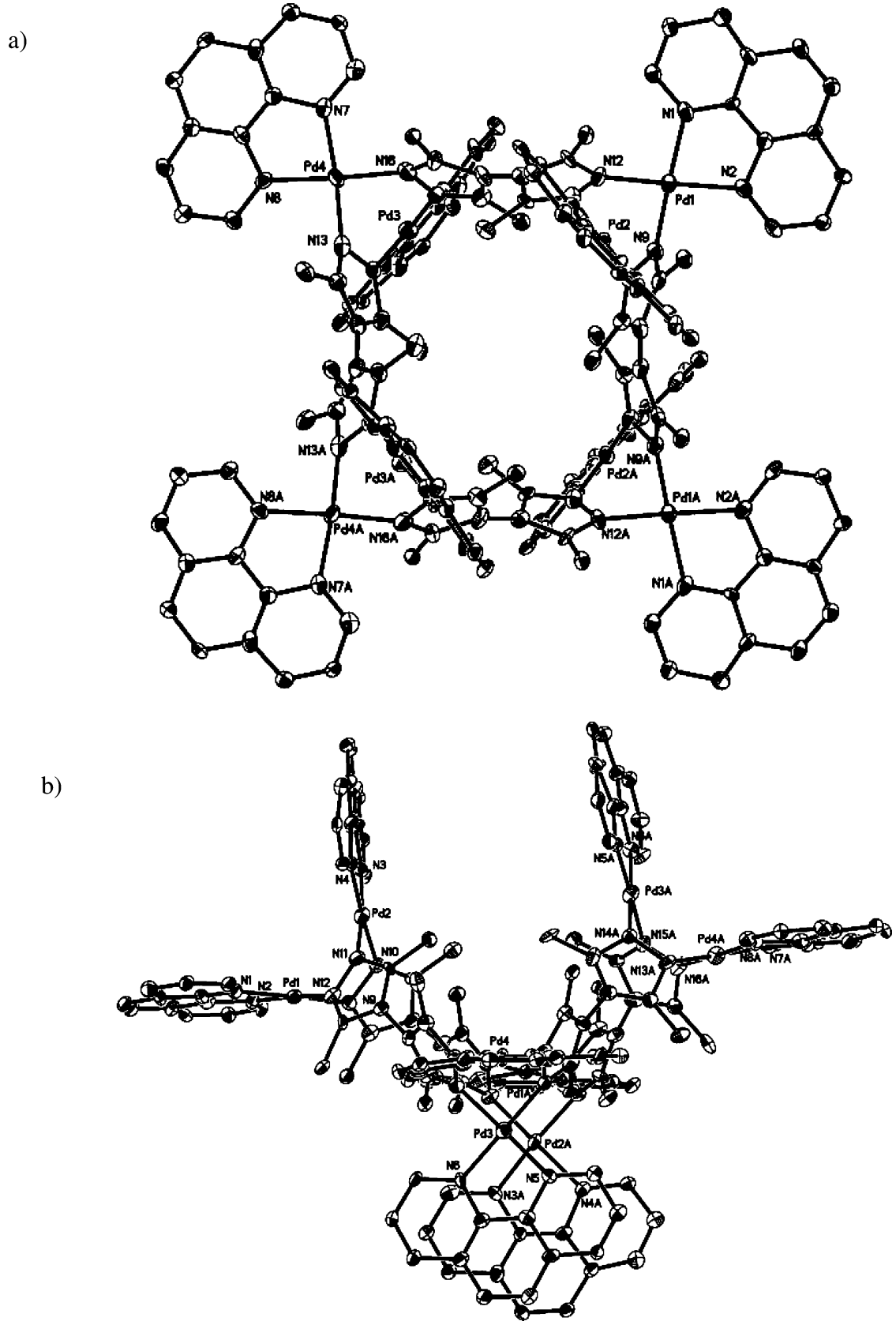

Figure 4. ORTEP diagram of the molecular structure of **3a**: (a) top view and (b) side view. Thermal ellipsoids are shown at the 30% probability level. The counterions and solvent molecules are omitted for clarity.

the spectrum. This NMR feature establishes that the geometry of the complex results in two different environments for the methyl groups caused by the highly distorted structure, as revealed by X-ray structure analysis of **1a** in the solid state. Similar phenomena also occurred in the ^{1}H NMR spectra of **2**, **3**, and **4**. As shown in Figure 1, the solution self-assembly

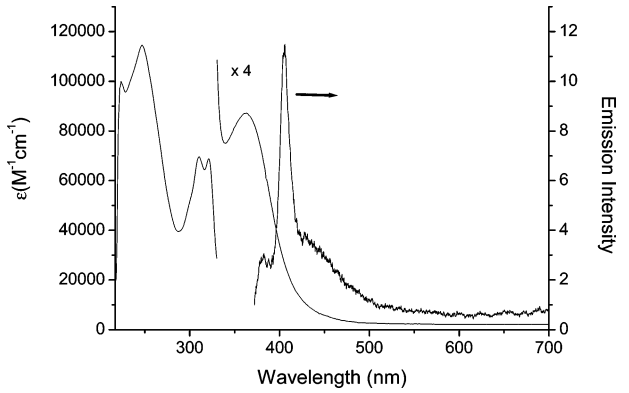

Figure 5. Absorption and emission spectra of **2** in methanol (6.0×10^{-6} M, 25 °C).

process of **1** was monitored by ^{1}H NMR complexation titration in D_2O. Upon addition of (bpy)Pd$(NO_3)_2$ to H_2L^1 in a 2:1 ratio, a clean NMR spectrum is observed which corresponds to a well-defined complex (Figure 1c).

CSI-MS spectra of **1** and **3** (in methanol), measured from a methanol solution, corroborated the $[(bpy)Pd]_8L^1_4$ and $[(phen)Pd]_8L^1_4$ compositions, respectively. As shown in Figure 2, the multiply charged molecular ions of **3** observed at m/z = 1709.1, 1118.5, 823.2, 646.3, 527.7, 443.6, and 380.6 correspond to the cations of $[\mathbf{3} - 2NO_3^-]^{2+}$, $[\mathbf{3} - 3NO_3^-]^{3+}$, $[\mathbf{3} - 4NO_3^-]^{4+}$, $[\mathbf{3} - 5NO_3^-]^{5+}$, $[\mathbf{3} - 6NO_3^-]^{6+}$, $[\mathbf{3} - 7NO_3^-]^{7+}$, and $[\mathbf{3} - 8NO_3^-]^{8+}$, respectively. Similarly, the multiply charged molecular ions of **1** observed at m/z = 1612.4, 1054.1, 774.9, 608.2, 495.8, 416.4, and 357.1 are assigned to the cations of $[\mathbf{1} - 2NO_3^-]^{2+}$, $[\mathbf{1} - 3NO_3^-]^{3+}$, $[\mathbf{1} - 4NO_3^-]^{4+}$, $[\mathbf{1} - 5NO_3^-]^{5+}$, $[\mathbf{1} - 6NO_3^-]^{6+}$, $[\mathbf{1} - 7NO_3^-]^{7+}$, and $[\mathbf{1} - 8NO_3^-]^{8+}$, respectively.

ESI-MS spectra of **2** and **4** in a methanol solution allowed the unambiguous assignment of the $[(bpy)Pt]_8L^1_4$ and $[(phen)Pt]_8L^1_4$ compositions, respectively. For example, the multiply charged molecular ions of **2** at m/z = 1290.9 $[\mathbf{2} - 3NO_3^-]^{3+}$, 952.7 $[\mathbf{2} - 4NO_3^-]^{4+}$, 749.8 $[\mathbf{2} - 5NO_3^-]^{5+}$, and 614.5 $[\mathbf{2} - 6NO_3^-]^{6+}$ and **4** at m/z = 1355.0 $[\mathbf{4} - 3NO_3^-]^{3+}$, 1000.7 $[\mathbf{4} - 4NO_3^-]^{4+}$, 788.2 $[\mathbf{4} - 5NO_3^-]^{5+}$, and 646.5 $[\mathbf{4} - 6NO_3^-]^{6+}$ were observed (see Supporting Information).

An ORTEP representation of the molecular structure of **1a**·$8H_2O$ is shown in Figure 3. Complex **1a** crystallizes in the monoclinic space group $C2/c$ with eight cocrystallized water molecules. It displays an interesting highly distorted tetragonal metallomacrocyclic structure with four (μ-pyrazolato-N,N')$_2$ doubly bridged $[(bpy)Pd]_2$ corners. There are no $\pi-\pi$ stacking interactions between the (bpy)Pd planes within each corner because of the large dihedral angles (78.1 and 85.7°). The separations of Pd1···Pd2 [3.215(1) Å] and Pd3···Pd4 [3.238(1) Å] are near the sum of the van der Waals radii of palladium (the typical value is 1.6 Å), which reveals quite weak Pd···Pd interactions.[21,27] The novel distorted structure results from the dramatic distortion of the bridging ligands. The interplanar angles of the bipyrazolyl ligand are in the range of 58−60° as a result of the steric repulsion of the four methyl groups.[23,24] Interestingly, the (bpy)Pd2, (bpy)-Pd4, (bpy)Pd4A, and (bpy)Pd2A planes are placed in the same environment along the procumbent direction, presenting an alternate arrangement, while the (bpy)Pd1, (bpy)Pd3, (bpy)Pd3A, and (bpy)Pd1A planes are located in the perpendicular direction with an alternate (up, down, up, down) conformation, which defines a cavity. In addition, eight methyl groups are located inside the cavity, and another eight methyl groups are outside the cavity. These structural features result in the two sets of observed resonances for the CH_3 groups in the ^{1}H NMR spectrum of **1**. The (bpy)-Pd1 and (bpy)Pd3A planes [or (bpy)Pd3 and (bpy)Pd1A planes] are almost parallel with a Pd···Pd separation of 8.910 Å. The most fascinating feature of the structure is the binding of one BF_4^- ion into the cavity by hydrogen bonds between C51−H51A and F23, between C60−H60B and F23, and between C41−H41B and F24. The contact parameters of these hydrogen bonds are H51A···F23, 2.42 Å; C51···F23, 3.15 Å; C51−H51A···F23, 132.8°; H60B···F23, 2.27 Å; C60···F23, 2.97 Å; C60−H60B···F23, 129.5°; H41B···F24, 2.33 Å; C41···F24, 3.23 Å; and C41−H41B···F24, 156.1°, respectively. Moverover, one water molecule is also included in the middle of the cavity. In the crystal, molecules of complex **1a** pack by weak intermolecular $\pi\cdots\pi$ stacking

Scheme 2

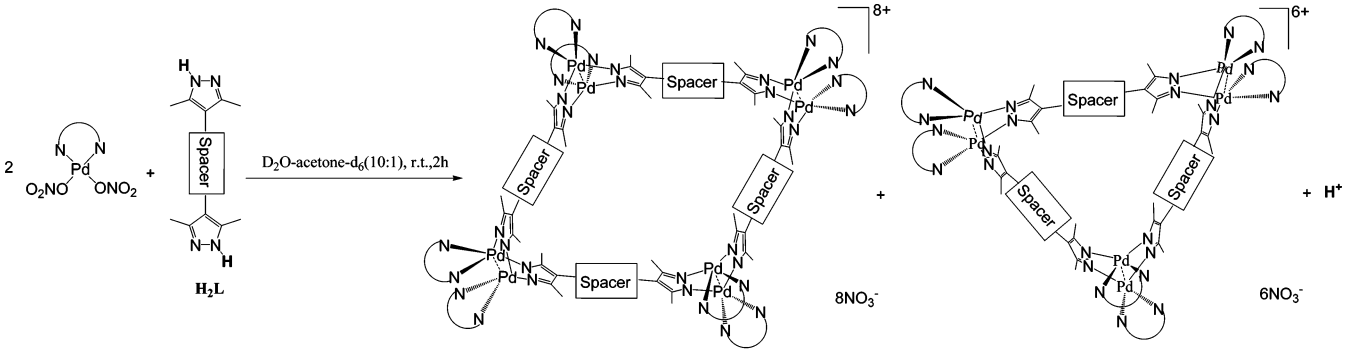

(bpy)Pd$(NO_3)_2$	H_2L^2	**5** 80%	**6** 20%
(phen)Pd$(NO_3)_2$	H_2L^2	**7** 75%	**8** 25%
(bpy)Pd$(NO_3)_2$	H_2L^3	**9** 47%	**10** 53%
(phen)Pd$(NO_3)_2$	H_2L^3	**11** 47%	**12** 53%

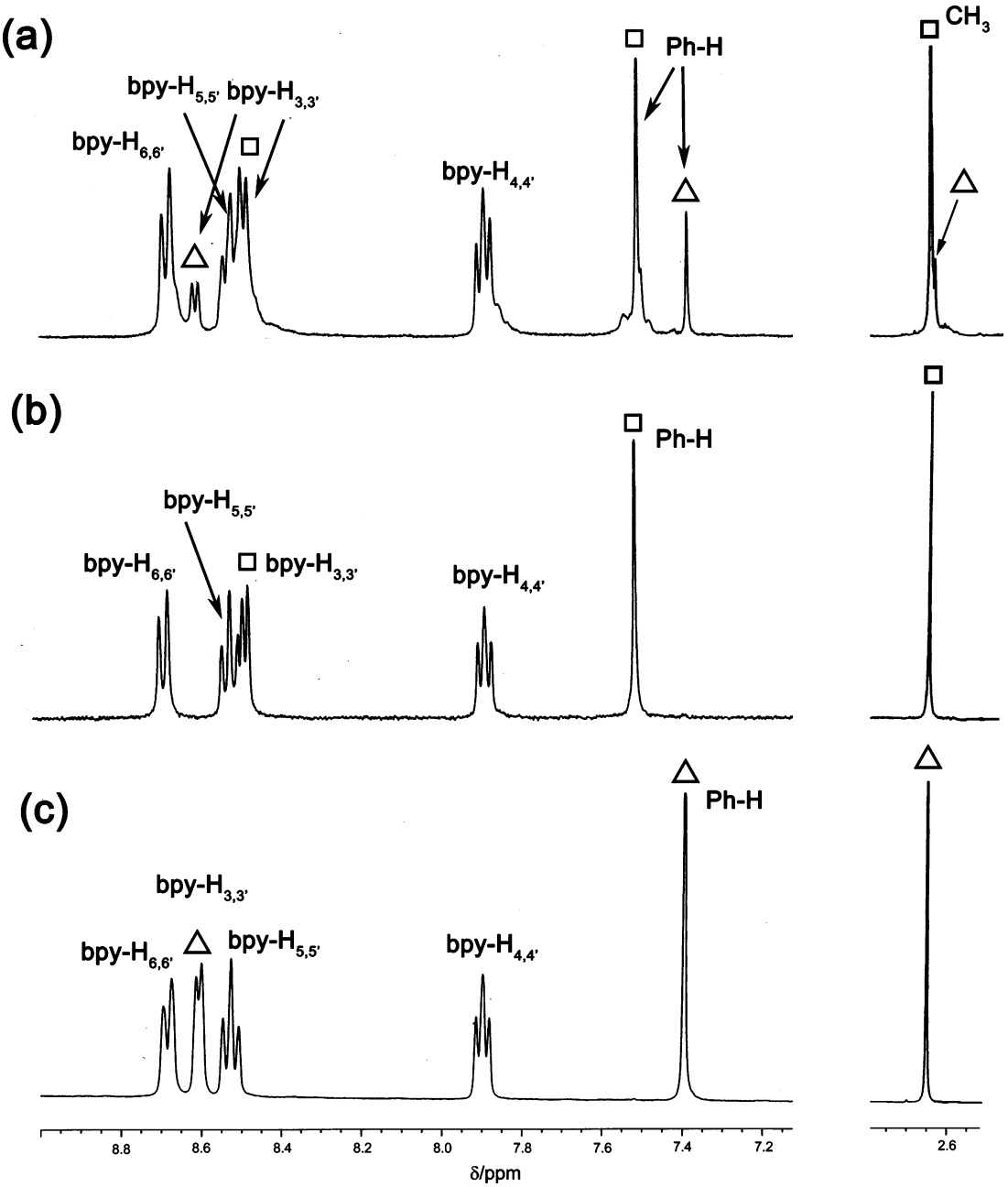

Figure 6. ^{1}H NMR spectra of **5** and **6** in the aromatic region (left, enlarged) and methyl region (right): (a) the mixture of **5** (80%) and **6** (20%) in the original self-assembling solution, (b) pure **5**, and (c) pure **6** (10:1 D_2O/acetone-d_6, 25 °C, TMS, □ and △ marking the characteristic peaks of **5** and **6**, respectively).

interactions involving two bpy rings between neighboring molecules with a contact distance of 3.886 Å.

An ORTEP representation of **3a**·13H_2O is shown in Figure 4. **3a** crystallizes in the monoclinic space group *P*2/*c*. The crystal structure of **3a** also displays a distorted tetragonal metallomacrocyclic structure with four (μ-pyrazolato-*N*,*N*′)$_2$ doubly bridged [(phen)Pd]$_2$ dimetal corners similar to that of **1a**. The dihedral angles between the phen ligands within each dimetal corner are 88.6 and 96.6°, which are significantly larger than those of **1a**. The separations of Pd1···Pd2 [3.239(1) Å] and Pd3···Pd4 [3.271(1) Å] are comparable to those of **1a** and also indicate weak Pd···Pd interactions. The interplanar angles of the bipyrazolyl ligand are in the range of 58−73°. The (phen)Pd2 and (phen)Pd3A planes [or (phen)Pd3 and (phen)Pd2A planes] are almost parallel (with the Pd···Pd separation of 8.264 Å) and, thus, form a cavity. Several water molecules are included in the cavity, but no PF_6^- counterion is found inside the cavity. In the crystal, complex **3a** stacks by intermolecular $\pi\cdots\pi$ stacking interactions involving two phen rings between neighboring molecules with the contact distance of 3.453 Å.

The UV−vis absorption and emission spectra for **1**−**4** were measured (Table 2). In the absorption spectrum of **2** (Figure 5), a characteristic vibronic structure of the diimine-centered LL transition, $^1(\pi \rightarrow \pi_1^*)$, lies near 300−330 nm. The band occurring near 250 nm is assigned to a higher-energy spin-allowed LL transition, $\pi \rightarrow \pi_2^*$, centered on the bipyridyl ligand. Analogous features are observed in the

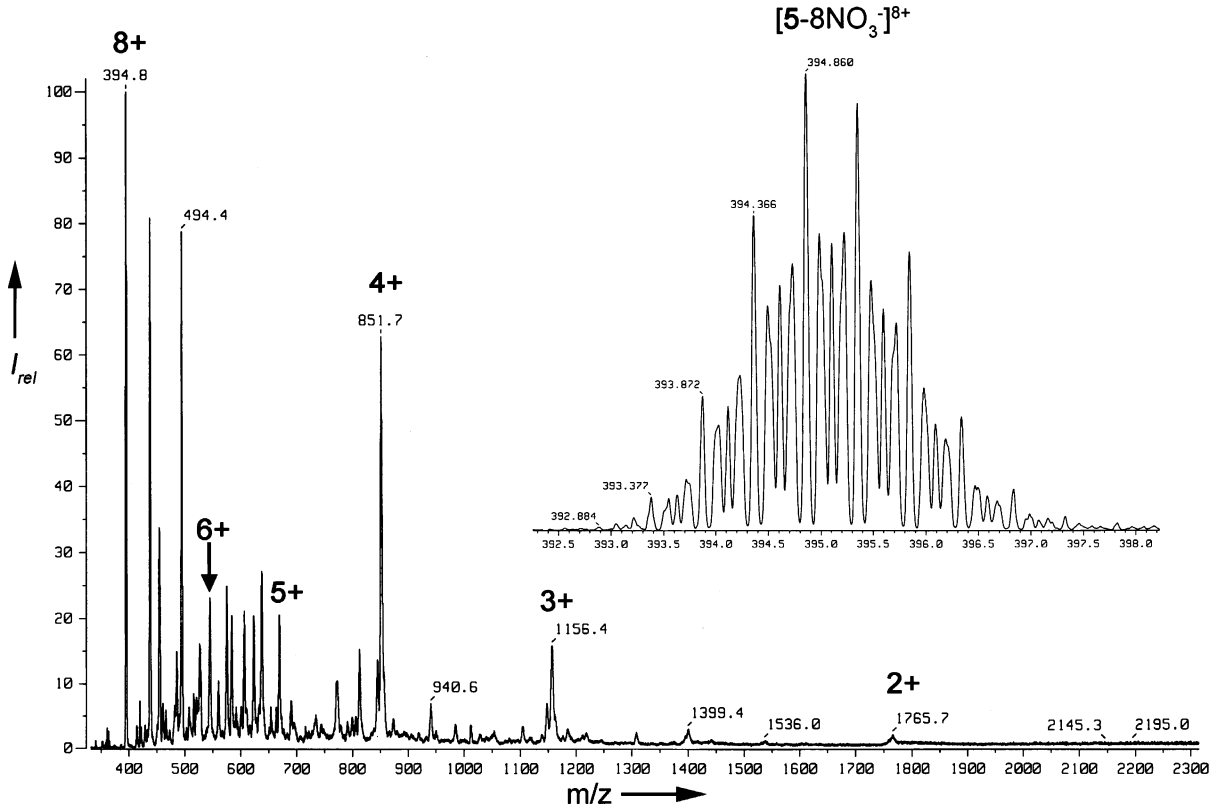

Figure 7. CSI-MS spectrum of **5** in methanol; the inset shows the isotopic distribution of the species $[\mathbf{5} - 8NO_3^-]^{8+}$.

Table 2. UV−Visible Spectroscopic Data (λ, nm) for Complexes **1**−**4** in Methanol [ϵ, M^{-1} cm^{-1}]

compound	$^1(\pi \rightarrow \pi_2^*)$	$^1(\pi \rightarrow \pi_1^*)$	^{1}MLCT	^{3}MLCT
1	237 [181 900]	309, 321(sh) [87 220, 71 830]	364, 383 [8930, 4800]	
2	247 [114 580]	311, 321 [69 430, 68 830]	363 [21 780]	420(sh) [3650]
3	222 [411 320]	275 [261 240]	353, 383 [31 420, 12 540]	
4	225 [251 760]	276 [204 320]	361, 372 [26 680, 29 060]	420(sh) [2680]

spectra of (bpy)$PtCl_2$ and (bpy)Pt(dmpz)$_2$ (where dmpz = 3,5-dimethylpyrazole).[31] At longer wavelengths (340−500 nm), similar to literature assignment,[31] the moderately intense lower-energy bands in the range 340−420 nm are assigned to ^{1}metal-to-ligand charge transfer [^{1}MLCT; d(Pt) $\rightarrow$ π^*-(bpy)] transitions, and the weak absorption tails at 410−500 nm are attributed to a transition to the corresponding triplet state. The emission spectrum of **2** in methanol solution that occurs upon excitation at 362 nm (Figure 5) shows an emission maximum at 406 nm that originates from the ^{1}-MLCT [d(Pt) $\rightarrow$ π^*(bpy)] state. The intense band near 362 nm in the excitation spectra of **2** in a methanol solution is in good agreement with the room-temperature solution absorption spectra.

Self-Assembly of $[M_8L_4]^{8+}$- and $[M_6L_3]^{6+}$-Type Crown-Shaped Macrocycles Based on Bipyrazole Ligands H_2L^2 and H_2L^3. As shown in Scheme 2, simply mixing (bpy)Pd-$(NO_3)_2$ with the immiscible bipyrazole ligand H_2L^2 in a 2:1 molar ratio in a 10:1 D_2O/acetone-d_6 solution at room temperature affords the mixture of bipyrazolate-bridged metallomacrocyclic complexes $\{[(bpy)Pd]_8L^2_4\}(NO_3)_8$ (**5**, 80%) and $\{[(bpy)Pd]_6L^2_3\}(NO_3)_6$ (**6**, 20%) in quantitative total yield with spontaneous deprotonation of the bipyrazole ligands at room temperature. Compounds **5** and **6** can be separated by repeated recrystallizations, as evidenced by ^{1}H and ^{13}C NMR spectra. The assignments of product **5** as $[M_8L_4]^{8+}$-type and **6** as $[M_6L_3]^{6+}$-type macrocycles are based on CSI-MS studies, where multiply charged intact molecular ions corresponding to cyclic tetramers and trimers were observed. Compounds **5a** and **6a** (PF_6^- salts of **5** and **6**) were obtained by exchange with a 10-fold excess of KPF_6 in aqueous solution. Single crystals of **5a** and **6a** were obtained by the vapor diffusion of diethyl ether into their acetonitrile solutions. X-ray crystal structures of **5a** and **6a** revealed the $[M_8L_4]^{8+}$-type and $[M_6L_3]^{6+}$-type macrocycles.

The solution of the 2:1 mixture of (bpy)Pd to L^{2-} in 10:1 D_2O/acetone-d_6 was measured by ^{1}H NMR spectroscopy (Figure 6a). Notably, only two singlets are observed in the aromatic region at 7.50 and 7.38 ppm (left, enlarged), which correspond to the two assemblies (**5** and **6**) in the solution, with yields of about 80 and 20%, respectively. In addition, the corresponding resonances of the two types of methyl groups appear in the upfield region (right), which reveal a 0.02 ppm shift from **5** to **6**. The characteristic peaks of **5** and **6** are denoted with □ and Δ, respectively. Furthermore, the signals that appear in the downfield region reflect the

(31) Connick, W. B.; Miskowski, V. M.; Houlding, V. H.; Gray, H. B. *Inorg. Chem.* **2000**, *39*, 2585−2592.

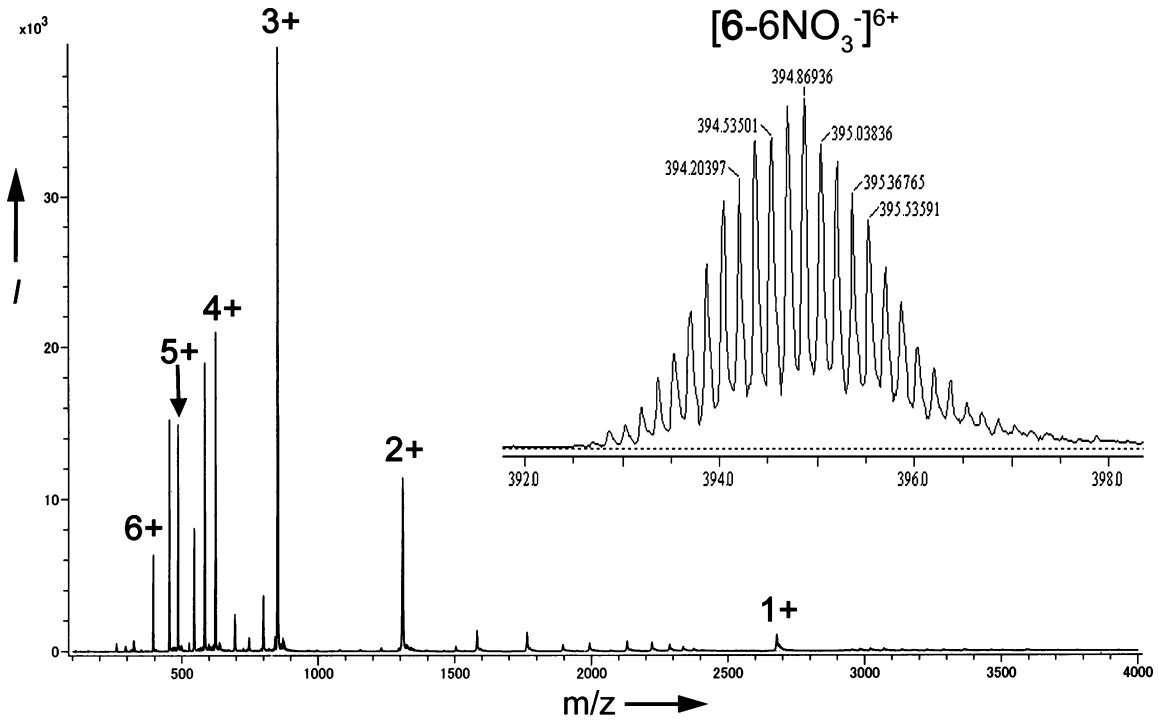

Figure 8. CSI-MS spectrum of **6** in methanol; the inset shows the isotopic distribution of the species $[\mathbf{6} - 6NO_3^-]^{6+}$.

proportions of the protons of the two types of bpy of **5** and **6**, respectively.

The well-resolved ^{1}H NMR spectra of the pure products **5** (Figure 6b) and **6** (Figure 6c) match the signals appearing in the spectrum of the mixture (Figure 6a). Importantly, the characteristic resonances of the benzene protons of L^{2-} in **5** and **6** are present at 7.50 ppm in Figure 6b and at 7.38 ppm in Figure 6c, respectively, which is completely identical to the corresponding resonances shown in Figure 6a. Integration of these signals indicates a 4:1 ratio, as shown in Scheme 2.

CSI-MS experiments provide strong evidence for the formation of $\{[(bpy)Pd]_8L^2_4\}(NO_3)_8$ (**5**) and $\{[(bpy)Pd]_6L^2_3\}(NO_3)_6$ (**6**). In the CSI-MS spectrum for **5** (Figure 7), the peaks appearing at m/z = 1765.7, 1156.4, 851.7, 669.0, 547.7, 461.0, and 394.8 can be assigned to $[\mathbf{5} - 2NO_3^-]^{2+}$, $[\mathbf{5} - 3NO_3^-]^{3+}$, $[\mathbf{5} - 4NO_3^-]^{4+}$, $[\mathbf{5} - 5NO_3^-]^{5+}$, $[\mathbf{5} - 6NO_3^-]^{6+}$, $[\mathbf{5} - 7NO_3^-]^{7+}$, and $[\mathbf{5} - 8NO_3^-]^{8+}$, respectively. Similarly, in the CSI-MS spectrum for **6** (Figure 8), the peaks appearing at m/z = 1308.1, 851.4, 622.8, 485.8, and 394.9 are attributed to $[\mathbf{6} - 2NO_3^-]^{2+}$, $[\mathbf{6} - 3NO_3^-]^{3+}$, $[\mathbf{6} - 4NO_3^-]^{4+}$, $[\mathbf{6} - 5NO_3^-]^{5+}$, and $[\mathbf{6} - 6NO_3^-]^{6+}$, respectively.

The ORTEP representations of **5a** and **6a** are depicted in Figures 9 and 10 , respectively. As shown in Figure 9, the crystal structure analysis for **5a** revealed the Pd_8 crown-shaped metallomacrocyclic structure with four (μ-pyrazolato-N,N')$_2$ doubly bridged $[(bpy)Pd]_2$ dimetal corners. In the dipalladium corners, the dihedral angles, defined by the N9−N10−Pd2−Pd1 plane and the N15A−N16A−Pd1−Pd2 plane or the N11−N12−Pd4−Pd3 plane and the N13−N14−Pd4−Pd3 plane, are 98.3 and 100.3°, respectively, which are significantly larger than those found in the reported molecular squares with dimetal corners (about 90°).[3] The dihedral angles between the two pyrazolate planes in the dipalladium corners are 82.8 (Pd1Pd2 corner) and 92.9° (Pd3Pd4 corner). This leads to the nearly square metallomacrocyclic structure with a significantly large cavity with dimensions of 13.5 × 13.5 Å, as defined by the distances between adjacent dipalladium centers. In the cavity, two acetonitrile molecules and several water molecules are found. All PF_6^- counterions are outside the cavity and are located near the dipalladium corners. Other solvent molecules are disordered, and most of the cavity space is empty. This void space leads to the very low density of 1.051 g cm^{-3} observed for **5a**. The dihedral angles between the bpy ligands within the dimetal corners are 65.6 [(bpy)Pd3 and (bpy)Pd4] and 73.8° [(bpy)Pd1 and (bpy)Pd2], which are obviously smaller than those of **1a** and **3a**. The separations of Pd1···Pd2 [3.1398(7) Å] and Pd3···Pd4 [3.1314(7) Å] are slightly shorter than the sum of the van der Waals radii of palladium, indicating the presence of weak Pd···Pd interactions. A side view of **5a** illustrates the crown conformation with the side length of the crown rims being about 22.0 Å and the cavity depth being about 8.5 Å. In the crystal, the molecules of **5a** stack by intermolecular $\pi\cdots\pi$ stacking interactions involving two bpy rings between neighboring molecules with a contact distance of 3.558 Å. Thus, long channels are formed by the packed cavities of complex **5a** along the *a* axis with a distance of 13.5 Å between diPd centers.

As shown in Figure 10, compound **6a** displays a crown-shaped trigonal macrocyclic structure with three (μ-pyrazolato-N,N')$_2$ doubly bridged $[(bpy)Pd]_2$ dimetal corners. In the dipalladium corners, the dihedral angles, defined by the N11−N12−Pd4−Pd3 plane and the N11A−N12A−Pd4−Pd3 plane or the N7−N8−Pd1−Pd2 plane and the N9−N10−Pd2−Pd1 plane, are 98.2 and 99.8°, respectively, which are comparable to those observed in **5a**. The dihedral angles between two pyrazolate planes in the dipalladium corners are 71.5 (Pd1Pd2 corner) and 79.4° (Pd3Pd4 corner),

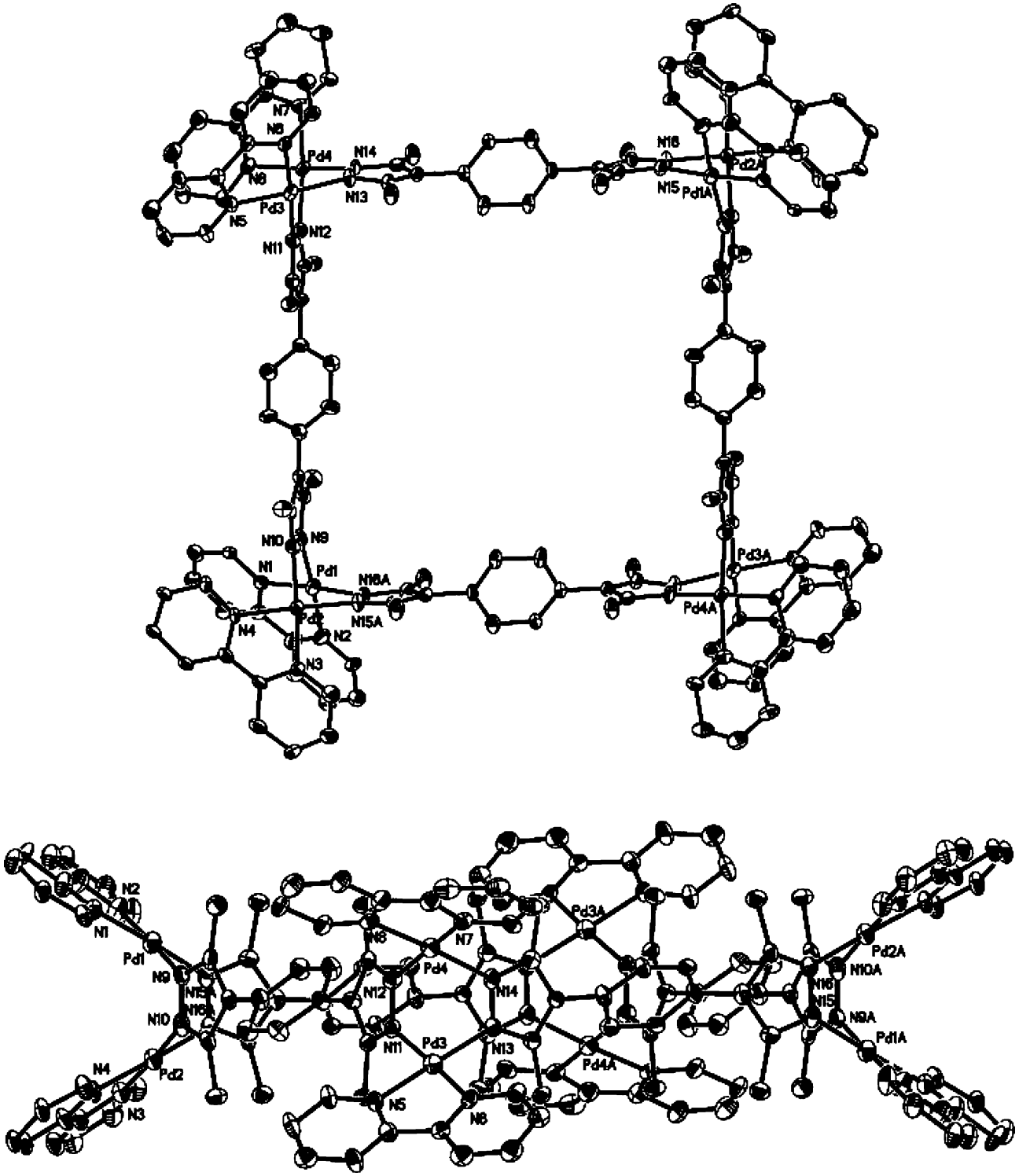

Figure 9. ORTEP diagram of the molecular structure of **5a** in top view (top) and side view (bottom). Thermal ellipsoids are shown at the 30% probability level. Counterions and solvent molecules are omitted for clarity.

which are notably smaller than those of **5a**. The midpoints of the diPd define a triangle with the average distance between vertexes being 13.3 Å. It is noteworthy that the conformation of the linkers, the three benzene rings, each forming a dihedral angle of about 45° with *pz* planes in the bipyrazole ligand, shows a syn, syn, syn orientation that leads to a crown-shaped trigonal metallomacrocyclic structure.

The dihedral angles between the bpy ligands within the dimetal corners are 73.3 [(bpy)Pd3 and (bpy)Pd4] and 88.9° [(bpy)Pd1 and (bpy)Pd2], which are slightly larger than those observed for **5a**. The separations of Pd1···Pd2 and Pd3···Pd4 are 3.2221(7) and 3.0990(9) Å, respectively, indicating weak Pd···Pd interactions. A side view of **6a** presents the crown conformation with the side length of the crown rims being about 23.0 Å and the cavity depth being about 9.0 Å. The packing of the triangular molecules in crystals of **6a** is also interesting (see Supporting Information): they are stacked in the crystal with alternating orientations differing

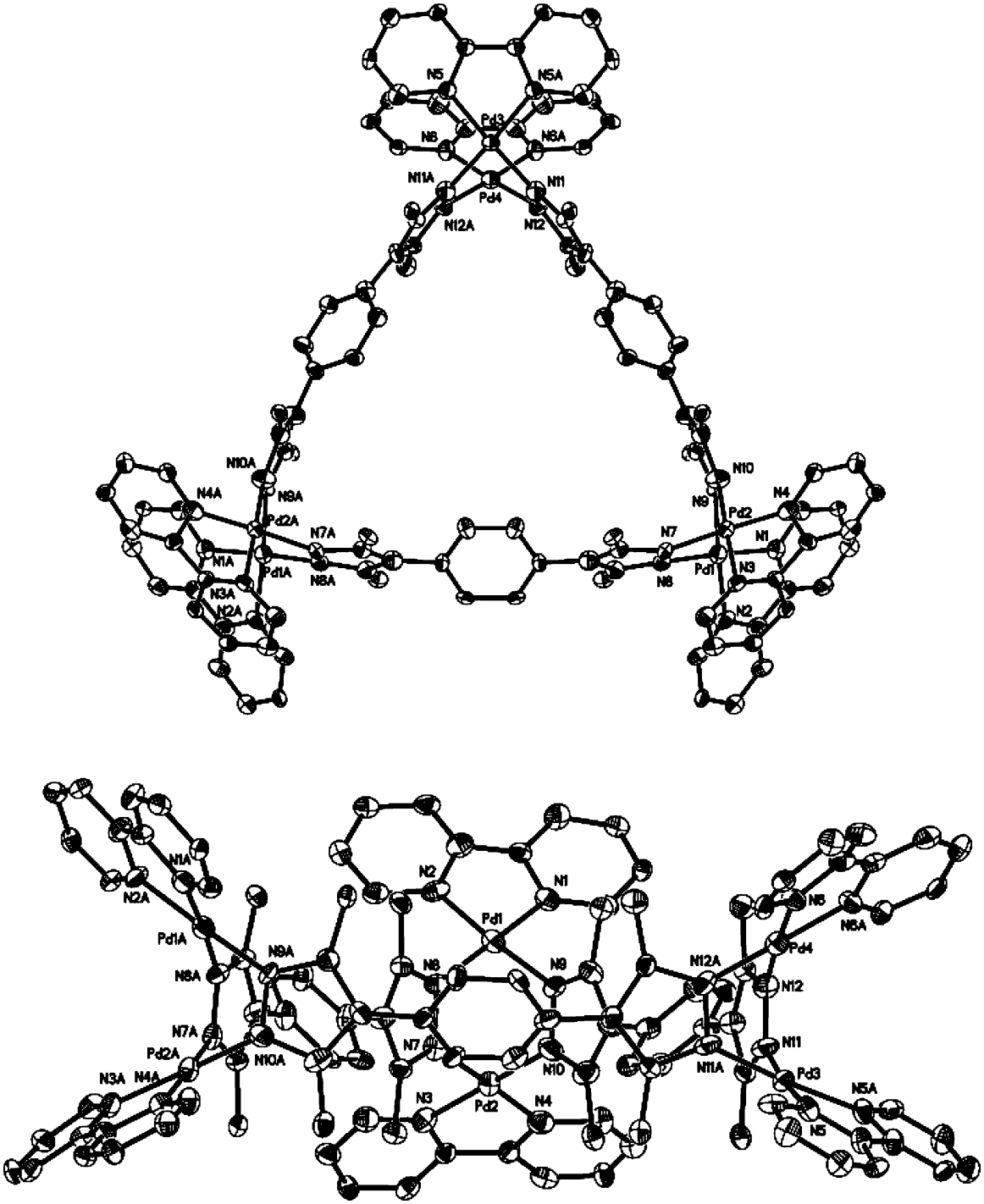

Figure 10. ORTEP diagram of the molecular structure of **6a** in top view (top) and side view (bottom). Thermal ellipsoids are shown at the 30% probability level. The counterions and solvent molecules are omitted for clarity.

by about 60°. Thus, a projection in the stacking direction has a hexagonal cross section, and the channel is filled with disordered PF_6^- counterions and water molecules.

As shown in Scheme 2, when (phen)Pd$(NO_3)_2$ and the immiscible bipyrazole ligand H_2L^2 are mixed in a 2:1 molar ratio in a 10:1 D_2O/acetone-d_6 solution, a mixture of bipyrazolate-bridged metallomacrocyclic complexes {[(phen)-Pd]$_8L^2{}_4$}$(NO_3)_8$ (**7**, 75%) and {[(phen)Pd]$_6L^2{}_3$}$(NO_3)_6$ (**8**, 25%) is formed in quantitative total yield with spontaneous deprotonation of the bipyrazole ligands. Compounds **7** and **8** can be separated by repeated recrystallizations, as monitored by their ^{1}H and ^{13}C NMR spectra. The assignments of product **7** as $[M_8L_4]^{8+}$-type and **8** as $[M_6L_3]^{6+}$-type macrocycles are based on CSI-MS studies. Attempts to grow crystals of **7** and **8** suitable for single-crystal X-ray structural evaluation were not successful.

The solution of the 2:1 (phen)Pd to L^{2-} coordination mixture in 10:1 D_2O/acetone-d_6 was measured by ^{1}H NMR spectroscopy (see Supporting Information). Notably, two singlets, at 7.64 and 7.50 ppm, due to the aromatic protons of L^{2-} are observed that correspond to the two assemblies **7** and **8** with yields of about 75 and 25%, respectively. In

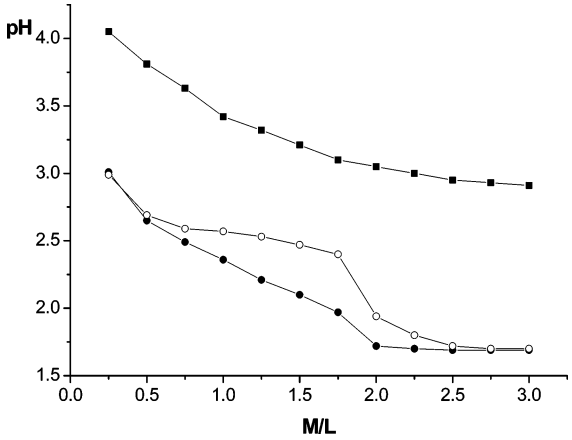

Figure 11. Plots of pH versus the M/L ratio in the self-assembly systems $\{[H_2L^2]_{initial} = 10$ mmol/L; ●, M = (bpy)Pd$(NO_3)_2$; ○, M = (phen)Pd$(NO_3)_2$; ■, M = (en)Pd$(NO_3)_2\}$.

addition, the corresponding resonances of the two different types of methyl groups appear in the upfield region, which reveal a 0.03 ppm shift from **7** to **8**. The well-resolved ^{1}H NMR spectra of the pure products **7** and **8** match the signals appearing in the spectra of the mixture.

ESI-MS and CSI-MS experiments allowed the unambiguous assignment of the two species $\{[(phen)Pd]_8L^2{}_4\}(NO_3)_8$ (**7**) and $\{[(phen)Pd]_6L^2{}_3\}(NO_3)_6$ (**8**; see Supporting Information). The peaks appearing at m/z = 1220.3, 899.5, 707.0, and 578.5 can be assigned to $[\mathbf{7} - 3NO_3^-]^{3+}$, $[\mathbf{7} - 4NO_3^-]^{4+}$, $[\mathbf{7} - 5NO_3^-]^{5+}$, and $[\mathbf{7} - 6NO_3^-]^{6+}$, respectively. Similarly, in the CSI-MS of **8**, the peaks appearing at m/z = 1380.5, 899.7, 659.0, 515.0, and 418.7 are attributed to $[\mathbf{8} - 2NO_3^-]^{2+}$, $[\mathbf{8} - 3NO_3^-]^{3+}$, $[\mathbf{8} - 4NO_3^-]^{4+}$, $[\mathbf{8} - 5NO_3^-]^{5+}$, and $[\mathbf{8} - 6NO_3^-]^{6+}$, respectively.

Remarkably, once formed, no interconversion between **5** and **6** (or **7** and **8**) could be detected by ^{1}H NMR in solution, probably a result of the strong bonding between the dimetal centers and the dianionic L^{2-} ligand. Furthermore, to assess the kinetic stability of the four complexes, **5** and **7** (or **6** and **8**) were combined in a 1:1 molar ratio in 1:2 D_2O/acetone-d_6 solution. These crossover experiments did not result in the formation of any new species, as indicated by the absence of any new signals in the NMR spectra (see Supporting Information). In contrast to the mononuclear cis-coordinated Pd(II) directed assemblies where an equilibrium exists between the squares and the triangles,[8] the four complexes described here (**5**−**8**) exhibit high kinetic stability in solution.

Figure 11 shows plots of pH versus M/L molar ratio in several self-assembly systems. Upon titration of M = (bpy)Pd$(NO_3)_2$ with H_2L^2 in a 10:1 water/acetone solution, the pH value sharply decreases to 1.72 at M/L = 2:1, indicating that the protons of H_2L have fully dissociated to form dianionic L^{2-} with the formation of the assemblies with the 2:1 (bpy)Pd to L^{2-} coordination. Similar results are observed for the titration of M = (phen)Pd$(NO_3)_2$ with H_2L^2. In contrast, when (en)Pd$(NO_3)_2$ (en = ethylenediamine) is used, the pH value decreases gently to near 3, and no deprotonated products were formed, as evidenced by ^{1}H NMR spectra and CSI-MS. In our recent work,[23] the combination of (en)Pd$(NO_3)_2$ and bipyrazole ligand can only form a single product of $\{[(en)Pd]_4L^1{}_4\}(NO_3)_4$ on the basis of ^{1}H and ^{13}C NMR spectra and single-crystal structure analysis. The titration results indicate that the aromatic ligand precoordinated metal center, (bpy)Pd or (phen)Pd, may behave as an electron acceptor to facilitate the deprotonation of 1*H*-bipyrazole.

Scheme 3

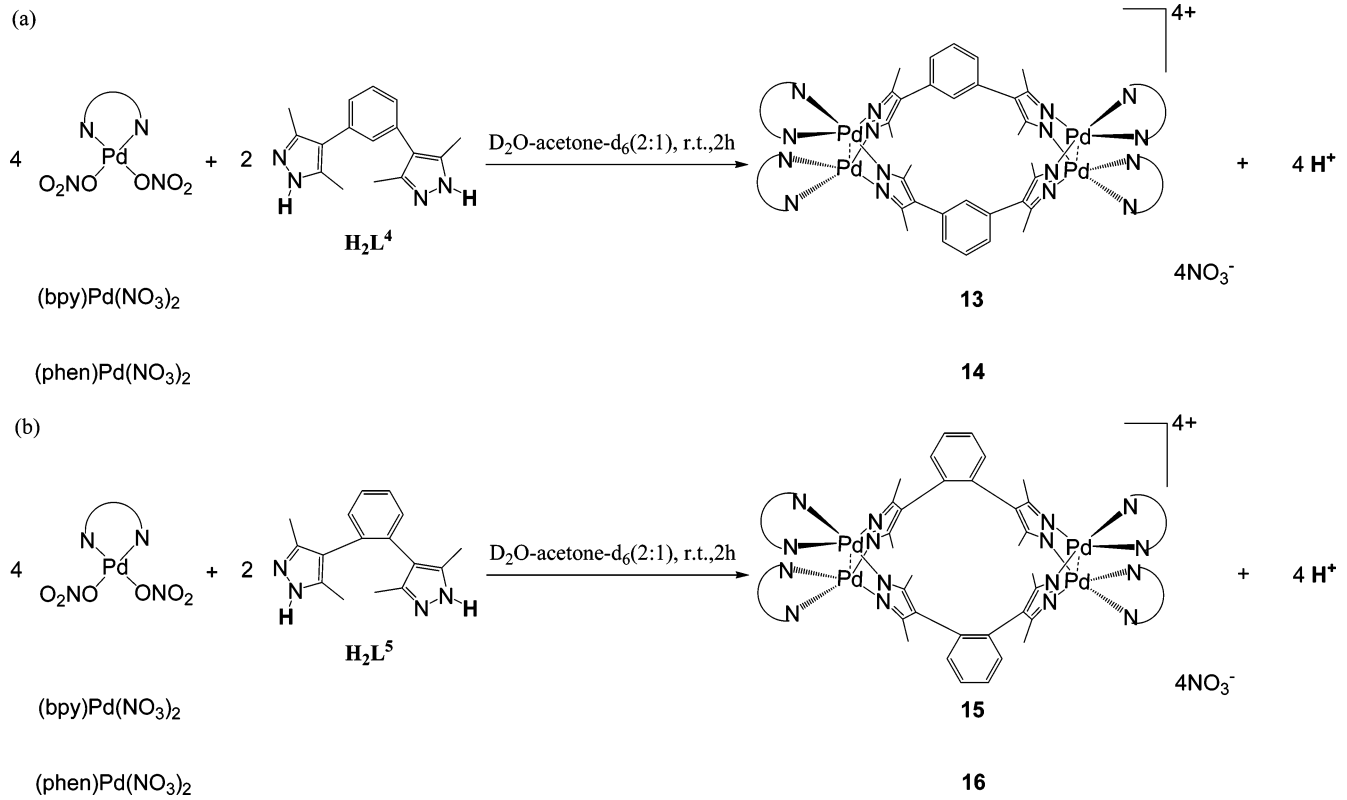

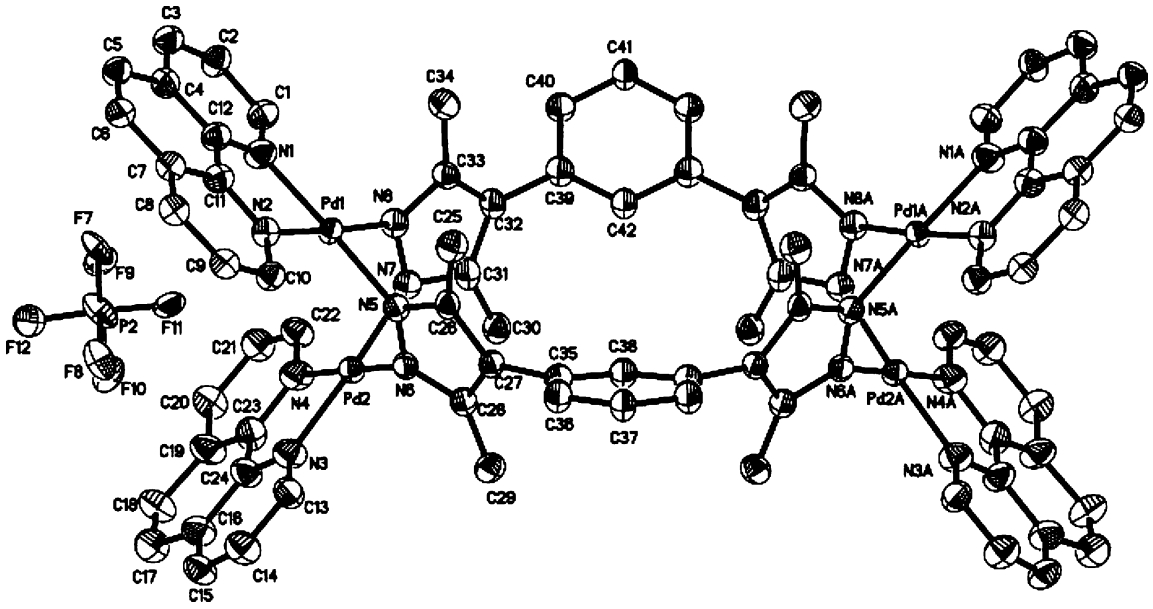

Figure 12. ORTEP diagram of the molecular structure of **14a**. Thermal ellipsoids are shown at the 30% probability level. The counterions and solvent molecules are omitted for clarity.

As shown in Scheme 2, when (bpy)Pd$(NO_3)_2$ [or (phen)-Pd$(NO_3)_2$] and the immiscible bipyrazole ligand H_2L^3 are mixed in a 2:1 molar ratio in a 10:1 D_2O/acetone-d_6 solution, a mixture of bipyrazolate-bridged metallomacrocyclic complexes $\{[(bpy)Pd]_8L^3{}_4\}(NO_3)_8$ (**9**, 47%) and $\{[(bpy)Pd]_6L^3{}_3\}$-$(NO_3)_6$ (**10**, 53%) or $\{[(phen)Pd]_8L^3{}_4\}(NO_3)_8$ (**11**, 47%) and $\{[(phen)Pd]_6L^3{}_3\}(NO_3)_6$ (**12**, 53%) is formed in quantitative yield with spontaneous deprotonation of the bipyrazole ligands at room temperature, as monitored by their ^{1}H NMR spectra. The assignments of products **9** and **11** as $[M_8L_4]^{8+}$-type and **10** and **12** as $[M_6L_3]^{6+}$-type macrocycles are based on CSI-MS and ESI-MS studies.

CSI-MS and ESI-MS allowed the unambiguous assignment of the species present in the mixture of **9** and **10** (or **11** and **12**). These techniques have been used to assign the species present in the triangle−square equilibrium.[8d] In the CSI-MS spectrum of the mixture of **9** and **10** (see Supporting Information), the peaks appearing at m/z = 1422.7, 1258.0, 928.2, 730.0, 680.4, 598.2, 531.9, 503.6, and 433.0 are assigned to $[\mathbf{10} - 2NO_3^-]^{2+}$, $[\mathbf{9} - 3NO_3^-]^{3+}$, $[\mathbf{9} - 4NO_3^-]^{4+}$ and $[\mathbf{10} - 3NO_3^-]^{3+}$, $[\mathbf{9} - 5NO_3^-]^{5+}$, $[\mathbf{10} - 4NO_3^-]^{4+}$, $[\mathbf{9} - 6NO_3^-]^{6+}$, $[\mathbf{10} - 5NO_3^-]^{5+}$, $[\mathbf{9} - 7NO_3^-]^{7+}$, and $[\mathbf{9} - 8NO_3^-]^{8+}$ and $[\mathbf{10} - 6NO_3^-]^{6+}$, respectively. Similarly, in the CSI-MS spectrum of the mixture of **11** and **12** (see Supporting Information), the peaks appearing at m/z = 975.1, 768.1, 716.3, 629.8, 560.3, 531.1, and 456.6 are attributed to $[\mathbf{11} - 4NO_3^-]^{4+}$ and $[\mathbf{12} - 3NO_3^-]^{3+}$, $[\mathbf{11} - 5NO_3^-]^{5+}$, $[\mathbf{12} - 4NO_3^-]^{4+}$, $[\mathbf{11} - 6NO_3^-]^{6+}$, $[\mathbf{12} - 5NO_3^-]^{5+}$, $[\mathbf{11} - 7NO_3^-]^{7+}$, and $[\mathbf{11} - 8NO_3^-]^{8+}$ and $[\mathbf{12} - 6NO_3^-]^{6+}$, respectively.

Self-Assembly of $[M_4L_2]^{4+}$-Type Macrocyles Based on Bipyrazole Ligands H_2L^4 and H_2L^5. Replacing the linear bipyrazole ligands with nonlinear bipyrazole ligands H_2L^4 and H_2L^5 clearly has the potential to yield different assemblies. The experimental findings (detailed below) are that looplike tetranuclear metallomacrocycles are formed. As shown in Scheme 3, suspension of (bpy)Pd$(NO_3)_2$ or (phen)-Pd$(NO_3)_2$ with bipyrazole ligands H_2L^4 or H_2L^5 in a 2:1 molar ratio resulted in complexes **13**, **14**, **15**, and **16**. The pure complexes were obtained in high yield by recrystallization from acetone and water. The formation of these four assemblies was supported by elemental analysis and ^{1}H and ^{13}C NMR spectroscopy. Single crystals of compound **14a** (PF_6^- as counteranions) and **15** were determined via X-ray crystallography and revealed the $[M_4L_2]^{4+}$-type macrocycles.

The ORTEP diagram of **14a** is shown in Figure 12. Complex **14a** crystallizes in the orthorhombic space group *Pnma* with 12 cocrystallized water molecules. The crystal structure analysis for **14a** revealed the Pd_4 bowl-shaped macrocyclic structure with two (μ-pyrazolato-*N*,*N*′)$_2$ doubly bridged [(phen)Pd]$_2$ dimetal corners. The two benzene rings, each forming a dihedral angle of about 63° with the *pz* planes in the bipyrazole-bridged ligand, show a syn, syn orientation according to the planes of (phen)Pd1 and (phen)Pd1A. The Pd1···Pd2 separation of 3.226 Å suggests the presence of weak metal−metal interactions. The remarkable structure feature is that the (phen)Pd1 and (phen)Pd2 planes (with a dihedral angle of 85.3°) form a cleft with a cavity size of approximately 8.5 Å (center-to-center distance). One PF_6^- binds between the two phen rings by anion−π interactions between the F7 atom and one phen ring, which are separated by 3.095 and 3.097 Å (F7···C11 and F7···C12), respectively.[32,33] The dihedral angle between the two *pz* planes at

(32) (a) Gamez, P.; van Albada, G. A.; Mutikainen, I.; Turpeinen, U.; Reedijk, J. *Inorg. Chim. Acta* **2005**, *358*, 1975−1980. (b) Rosokha, Y. S.; Lindeman, S. V.; Rosokha, S. V.; Kochi, J. K. *Angew. Chem., Int. Ed.* **2004**, *43*, 4650−4652. (c) Demeshko, S.; Dechert, S.; Meyer, F. *J. Am. Chem. Soc.* **2004**, *126*, 4508−4509. (d) de Hoog, P.; Gamez, P.; Mutikainen, H.; Turpeinen, U.; Reedijk, J. *Angew. Chem., Int. Ed.* **2004**, *43*, 5815−5817. (e) Quiñonero, D.; Garau, C.; Rotger, C.; Frontera, A.; Ballester, P.; Costa, A.; Deyà, P. M. *Angew. Chem., Int. Ed.* **2002**, *41*, 3389−3392. (f) Alkorta, I.; Rozas, I.; Elguero, J. *J. Am. Chem. Soc.* **2002**, *124*, 8593−8598. (g) Mascal, M.; Armstrong, A.; Bartberger, M. *J. Am. Chem. Soc.* **2002**, *124*, 6274−6276.

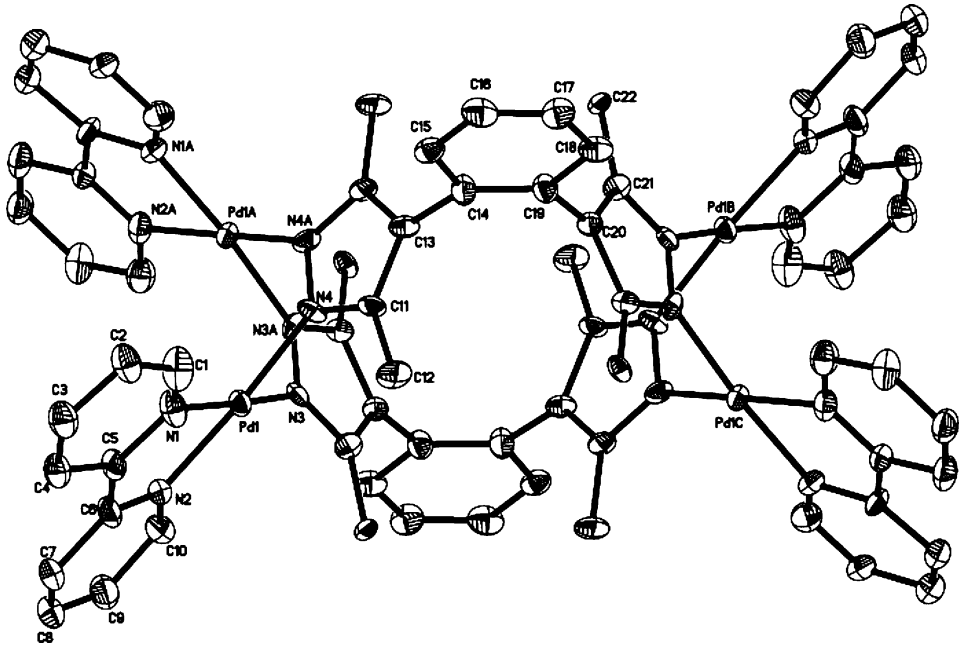

Figure 13. ORTEP diagram of the molecular structure of **15**. Thermal ellipsoids are shown at the 30% probability level. The counterions and solvent molecules are omitted for clarity.

each corner is 69.2°, which is smaller than the dihedral angle between the Pd1−N5−N6−Pd2 and Pd1−N7−N8−Pd2 planes (100.1°). The cavity of the Pd_4 bowl-shaped macrocycle is small. The distance between the two central phenyl rings is about 7.9 Å, and the distances of Pd1−Pd1A and Pd2−Pd2A are 11.0 and 10.2 Å, respectively, leaving no space for guest inclusion, as evidenced by the absence of PF_6^- counterions in the cavity. Instead, solvent molecules occupy the cavity. The Pd_4 bowl-shaped cationic macrocycles are stacked along the *c* axis to produce long channels with a distance of 10.4 Å between the Pd centers. Numerous water molecules are packed in the interlayers.

Single crystals of compound **15** were obtained by slow evaporation of its aqueous solution. Complex **15** crystallizes in the orthorhombic space group *Ibam* with eight cocrystallized water molecules. The crystal of compound **15** also displays a Pd_4 macrocyclic structure (Figure 13). The Pd(1)···Pd(1A) separation of 3.209 Å is comparable to that observed in **14a**. The dihedral angle between the two adjacent bpy rings is canted at 71.5°, notably smaller than that of **14a**, while the dihedral angle (93.8°) between the two *pz* planes in the corner is significantly larger than that of **14a**. The two phenyl planes are parallel to each other and perpendicular to the *pz* planes, caused by steric hindrance. Compound **15** forms a square cavity with a size of 5.4 × 5.4 Å, and one water molecule is included inside the cavity. The Pd_4 cationic macrocycles are stacked along the *c* axis to produce long channels with a distance of 11.1 Å between the phenyl planes. Numerous water molecules and all of the nitrate counterions are packed in the interlayers.

Conclusions

Bipyrazolate-bridged metallomacrocycles with dipalladium(II) or diplatinum(II) centers can be obtained in nearly quantitative yield from $(bpy)Pd(NO_3)_2$ [or $(bpy)Pt(NO_3)_2$, $(phen)Pd(NO_3)_2$, and $(phen)Pt(NO_3)_2$] and 1*H*-bipyrazolyl ligands in 2:1 molar ratio via a directed self-assembly process that occurs along with spontaneous deprotonation of the ligands. The assemblies have been characterized by ^1H and ^{13}C NMR, CSI-MS or ESI-MS, and UV−vis and luminescence spectroscopy in solution and, in the cases of **1**, **3**, **5**, **6**, **14**, and **15**, by single-crystal X-ray diffraction methods. In addition, the spontaneous deprotonation of H_2L in the solution self-assembly process was monitored by NMR and pH-complexation titration. This system represents a facile approach from mononuclear coordination motifs to supramolecular metallomacrocyles with dimetal coordination motifs.

Acknowledgment. This project was supported by National Natural Science Foundation of China (Nos. 90206013, 50373051). We thank Prof. Lyle D. Isaacs (University of Maryland) for reading the manuscript and for helpful discussions.

Supporting Information Available: ^1H NMR spectra of **7** and **8**, the 1:1 (molar ratio) mixture of **5** and **7**, the 1:1 (molar ratio) mixture of **6** and **8**; CSI-MS or ESI-MS spectra of **1**, **2**, **4**, **7**, **8**, **9**, **10**, **11**, and **12**; the absorption and emission spectra of **4**; tables of selected bond lengths and bond angles for **1a**, **3a**, **5a**, **6a**, **14a**, and **15**; packing diagrams of **5a**, **6a**, **14a**, and **15**; and X-ray crystallographic files, in CIF format, for complexes **1a**, **3a**, **5a**, **6a**, **14a**, and **15**. This material is available free of charge via the Internet at http://pubs.acs.org.

(33) Vilar, R. *Angew. Chem., Int. Ed.* **2003**, *42*, 1460−1477.

IC0509332